



## In-Depth Survey Report

---

# **ENGINEERING CONTROLS FOR NANO-SCALE GRAPHENE PLATELETS DURING MANUFACTURING AND HANDLING PROCESSES**

Li-Ming Lo, Ph.D.

Duane Hammond, M.S., P.E.

Isaac Bartholomew

Daniel Almaguer, M.S.

William Heitbrink, Ph.D., C.I.H.

Jennifer Topmiller, M.S.

---

**Division of Applied Research and Technology  
Engineering and Physical Hazards Branch  
EPHB Report No. 356-12a**

**December 2011**

**DEPARTMENT OF HEALTH AND HUMAN SERVICES  
Centers for Disease Control and Prevention  
National Institute for Occupational Safety and Health**



**Site Surveyed: Nanomaterial manufacturing facility, Midwestern USA**

**NAICS Code:**

**Survey Dates: September 29–30, 2010**

**Surveys Conducted By: Li-Ming Lo, NIOSH/DART/EPHB**

**Duane Hammond, NIOSH/DART/EPHB**

**Daniel Almaguer, NIOSH/DART/EPHB**

**Isaac Bartholomew, NIOSH/DART/EPHB**

**William Heitbrink, NIOSH/DART/EPHB**

**Employer Representatives  
Contacted**

**Contractor Representatives:**

## **Disclaimer**

The findings and conclusions in this report are those of the authors and do not necessarily represent the views of NIOSH. Mention of any company or product does not constitute endorsement by NIOSH. In addition, citations to websites external to NIOSH do not constitute NIOSH endorsement of the sponsoring organizations or their programs or products. Furthermore, NIOSH is not responsible for the content of these websites. All Web addresses referenced in this document were accessible as of the publication date.

## Table of Contents

Disclaimer.....	iii
Abstract.....	v
Background.....	1
Potential Health Effects of Engineered Nanographene Platelets .....	1
Published Regulations.....	2
Production Areas.....	3
Engineering Controls .....	4
Overview .....	6
Sampling Plan .....	7
Concentration Measurements of Area Samples.....	10
Examination of Airflow around Enclosure and Local Exhaust .....	12
Compressor.....	14
Refining Process .....	17
Product Harvesting .....	17
Raw Material Preparation.....	24
Post-Treatment Process .....	27
Tube Cooling and Insulator Removal .....	28
Effect of Tube Cooling Time .....	32
Non-Production Areas.....	33
R&D Laboratories .....	33
Offices .....	35
Refining Area.....	38
Post-Treatment Area .....	42
Non-Production Areas.....	44

## Abstract

This report summarizes the study results of an evaluation of engineering controls for manufacturing and handling graphene nanoplatelets in the workplace. Direct-reading instruments, the Fast Mobility Particle Sizer (FMPS) spectrometer, the Aerodynamic Particle Sizer (APS) spectrometer, a gravimetric aerosol monitor (DustTrak), and a black carbon monitor were used to provide real-time characterization of the airborne particle concentrations released from the processes in the production areas.

For the refining process, measurement results indicated that larger size particles (or agglomerated nanomaterials) at 2–3 micrometers ( $\mu\text{m}$ ) were released into the workplace. These critical tasks included raw material preparation, product harvesting, and product transfer. There was no control measure for material preparation and product harvesting. Product transfer was performed inside a ventilated enclosure operated at an average face velocity of 78 feet per minute (fpm).

Fume hoods and glove boxes were used in the laboratory areas. No noticeable particle emissions were measured by the direct-reading instruments when these control measures were used for research and development (R&D) activities.

In the post-treatment process, the tasks of tube cooling and insulator removal from tubes generated high concentrations with peak number concentrations higher than  $2 \times 10^6$  particles per cubic centimeter ( $\#/\text{cm}^3$ ); most of the particles were less than 15 nanometers (nm) in diameter. The test results also demonstrated that extending tube cooling time can lower nanoparticle concentrations released from this process. The existing local exhaust ventilation located on top of a reactor did not effectively reduce particle emissions, because of the low operating flow rate (96 cubic feet per minute, cfm) and no appropriate receiving hood to capture airborne contaminants.

Special attention should be paid to the high particle concentrations found in the non-production areas. The nanoparticle concentrations with peaks at 10 and 70 nm in the R&D laboratories were 19%–64% higher than the background concentrations found in the production areas ( $1 \times 10^4 \#/\text{cm}^3$ ). The results of particle size analysis for the office areas showed that the fine particles less than 560 nm were lognormally distributed at 25–40 nm in different locations.

Flexible enclosures are recommended to prevent releases during material preparation and product harvesting in the refining process. Higher air velocities are preferred to provide good containment during product transfer, though the average face velocity of the enclosure meets the recommended criteria from the Occupational Safety and Health Administration (OSHA) (60–100 fpm) and the American Conference of Industrial Hygienists (ACGIH) (75–100 fpm). Modifying the existing canopy hood or using an isolated work area (e.g., downflow booth) for the post-treatment process are also suggested to mitigate particle emissions. Because the particle concentrations in both the production areas and the non-production areas are on the same order of magnitude, using separate ventilation systems and maintaining a positive pressure for the non-production areas are recommended. A preferred pressure scheme of  $0.04 \pm 0.02$  inches of H<sub>2</sub>O [ACGIH, 2010] can improve air quality.

No specific regulatory occupational exposure limit (OEL) for nanographene platelets exists, but improved containment is recommended to lower potential risks associated with these nanomaterials. Installation of appropriate engineering controls in the workplace can protect workers during manufacturing and handling of the engineered nanomaterials.

## Introduction

### Background

This study, supported by the NIOSH Nanotechnology Research Center (NTRC), evaluated the effectiveness of control measures used by nanomaterial manufacturers. Workplace controls have been recommended to prevent or minimize exposure to engineered nanomaterials [Safe Work Australia, 2009b], because the potential risks associated with nanoparticle exposure from toxicological research of engineered nanomaterials have been reported [Buzea *et al.*, 2007; International Organization for Standardization, 2008; European Agency for Safety and Health at Work, 2009; Safe Work Australia, 2009a]. Engineering controls such as enclosures, fume hoods, glove boxes/bags, cleanrooms, laminar flow clean benches, and local exhaust ventilation have been adopted in nanomanufacturing workplaces [ICON, 2006]. Only limited data on the effectiveness of these engineering controls have been obtained to date. NIOSH is conducting field evaluations to gain practical information and provide recommendations on control measures for protecting workers from occupational exposure to nanoparticles. The study results will lead to increased understanding and better recommendations for nano-specific engineering controls during manufacturing and handling of nanomaterials in workplaces.

### Potential Health Effects of Engineered Nanographene Platelets

The company manufactures nanostructured graphene platelets (NGPs). NGPs are new types of nanoparticles made from graphite, and their typical dimensions are 0.34–100 nm in thickness and 0.5–20  $\mu\text{m}$  in length. NGPs are similar to carbon nanotubes (CNTs), but their thermal/mechanical properties and characteristics are superior to other carbon-based nanomaterials [Jang & Zhamu, 2008; Rafiee *et al.*, 2009]. Some promising applications of NGPs have been reported including storage of hydrogen for energy production [Heine *et al.*, 2004], composite thin films as electrical conductors [Watcharotone *et al.*, 2007], and electrodes for lithium ion batteries [Cheekati *et al.*, 2010].

Some research has been done for NGP applications in biosensing, drug delivery, and biological imaging, but the toxicological data on NGPs or NGP composites are limited. A research group conducted a long-term *in vivo* study of nanographene sheets intravenously administered to mice at 20 milligram per kilogram (mg/kg) for 3 months [Yang *et al.*, 2011]. The results showed that nanographene sheets did not cause appreciable toxicity to the

treated mice. These nanomaterials accumulated in the liver and spleen and were gradually cleared by excretion.

Workers may be exposed to NGPs by way of inhalation, dermal contact, ingestion, or injection during manufacturing and handling of the nanomaterials. Appropriate engineering controls can reduce emissions, providing protection for workers. In addition, personal protective equipment (PPE) such as masks/respirators, work suits, gloves, and safety glasses/goggles is strongly recommended when performing these tasks.

### **Published Regulations**

Currently, no regulatory occupational exposure limit (OEL) for engineered nanomaterials exists. The OSHA 8-hour total weight average (TWA) Permissible Exposure Limit (PEL) and ACGIH Threshold Limit Value (TLV) for carbon black is 3.5 milligram per cubic meter ( $\text{mg}/\text{m}^3$ ) [OSHA; ACGIH, 2011]. In the British Standards Institution guide [BSI, 2007], a benchmark exposure level (BEL) of 0.01 fiber per milliliter (fiber/mL) for insoluble fibrous nanomaterials (such as carbon nanotubes and nanowires) has been recommended.

## Manufacturing Facility and Control Measures

Two main production areas were located in this NGP manufacturing facility (**Figure 1**). The refining area was separated from other areas with flexible curtains and was equipped with two wall exhausts connected to the process tanks. The post-treatment area was an open space. General tasks performed by workers in the production areas included raw material preparation, mixing, transporting to production equipment, product harvesting, and product weighing and transferring into package containers.

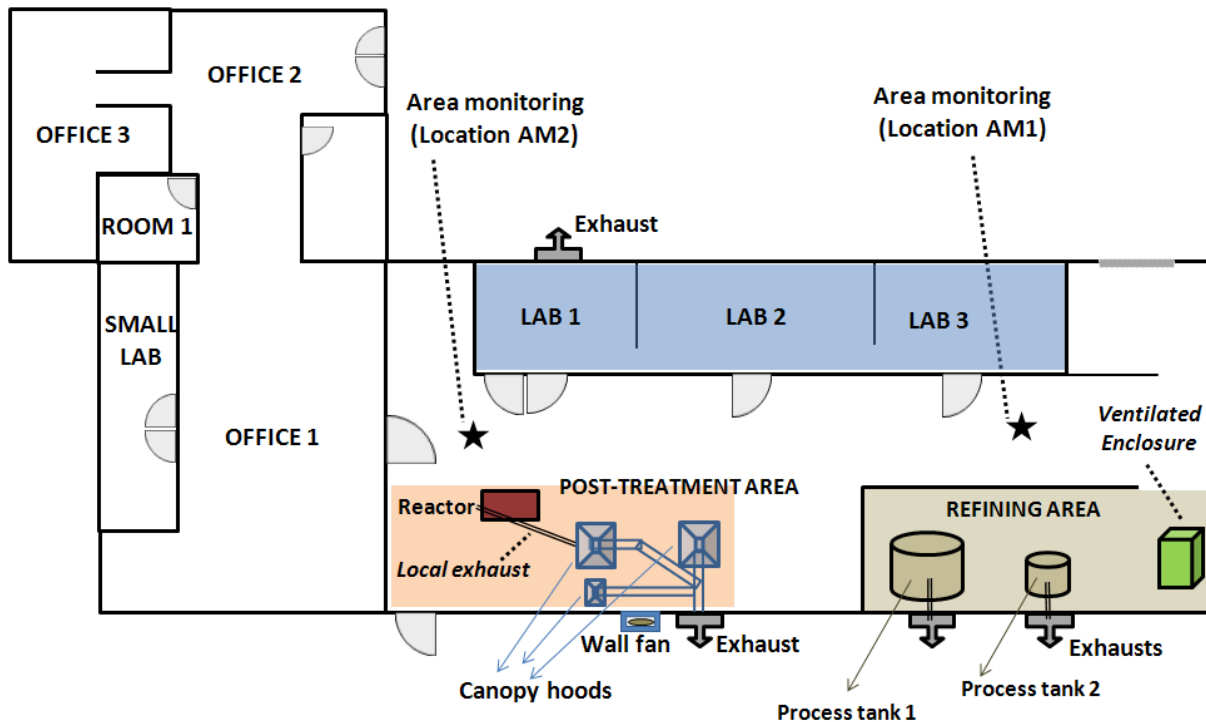


**Figure 1:** Layout of the study site. Two main production areas are highlighted in light orange and light tan. Star symbols show the locations for area monitoring during the survey.

### Production Areas

Two process tanks were used to produce different products in the refining area. Each tank had two stainless steel containers to collect the final products for different particle sizes (**Figure 2**). Large-sized nanomaterials were separated by Discharger 1 and collected in Container 1. Small-sized nanomaterials were deposited on Discharger 2 for product collection in

Container 2 by using a compressor near this production area. To prepare raw materials for the refining process, workers needed to remove materials from a drum and transferred them to a container on a scale for weighing, then mixed the materials with water inside a mixer. The post-treatment process was done in a reactor. In an open area, workers performed the task of product harvesting after cooling the process tubes and removing insulators at both ends of the tubes. In this study, three tubes were prepared for every test.

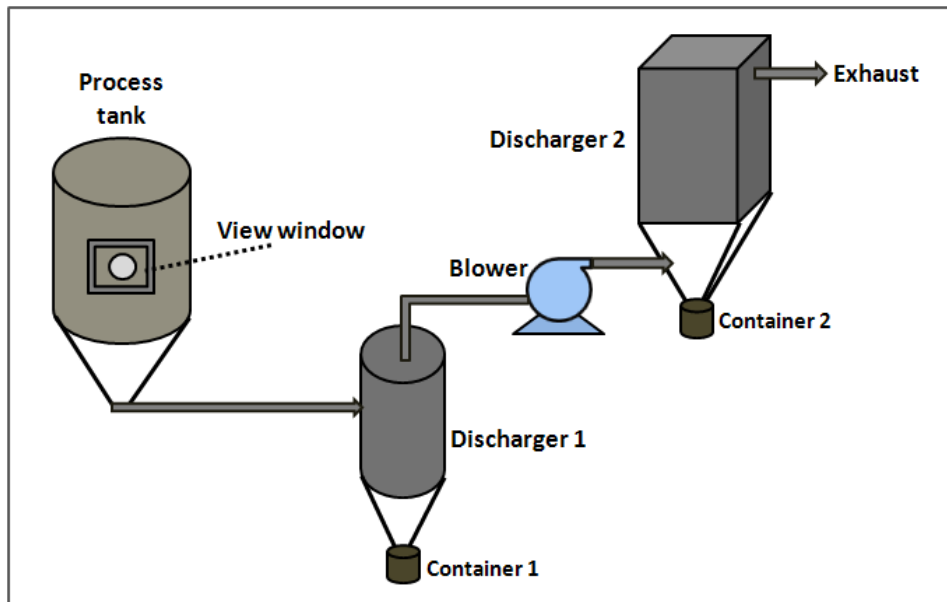


**Figure 2:** Diagram of the process tank.

### Engineering Controls

The refining process was performed without engineering controls, except for the use of a ventilated enclosure to control emissions during the final step of transferring and weighing of products. The enclosure was ventilated by a constant-speed fan, but its face velocity could be changed by raising or lowering the enclosure door. The enclosure door was usually fully open for easy access during use by workers (**Figure 3**). A regular fibrous filter panel was located on the top of the enclosure.



**Figure 3:** Ventilated enclosure used to weigh and transfer products in refining area.

In the post-treatment area, local exhaust ventilation (4" diameter flexible duct shown in **Figure 4**) was located on the top of the production reactor to mitigate nanoparticle emissions from the process. In addition, a 4.5 ft x 4.25 ft wall fan and three canopy hoods were installed in this area (**Figure 1** and **Figure 5**). This wall fan was turned on to remove contaminants while performing the post-treatment process. The local exhaust was simply connected to one of the hoods to exhaust the contaminants. Other canopy hoods shown were turned off during the survey.

In the laboratories, most research activities were conducted in hoods: fume hoods for product mixing and glove boxes for new product development. It was noted that a small laboratory was located in the office area where product development was performed in a glove box.



**Figure 4:** Local exhaust ventilation used in the post-treatment area.

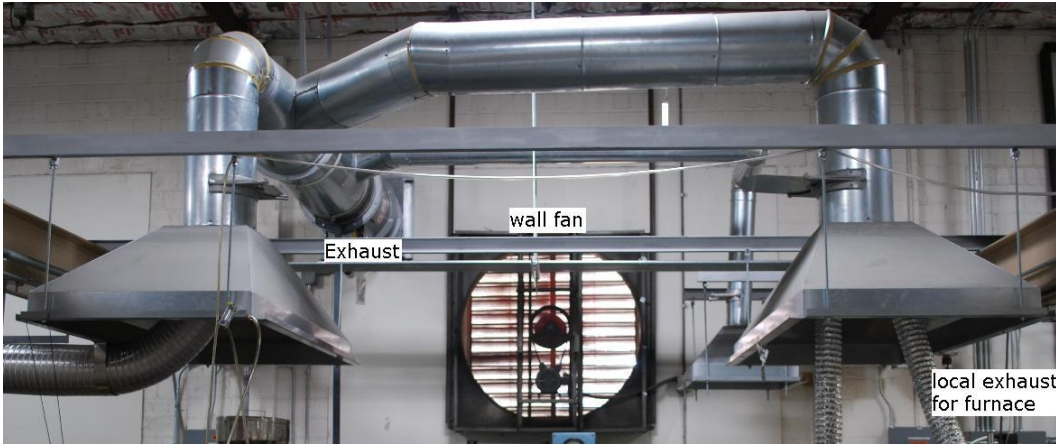


**Figure 5:** Wall fan and canopy hoods in the post-treatment area.

## Methodology

### Overview

The area samples were collected at two locations named AM1 and AM2 shown in **Figure 1** to check general air quality of the facility and help identify sources releasing engineered nanomaterials. In addition, the airborne particle concentrations in the non-production areas, including offices and laboratories, were monitored by the instruments to check the overall air quality. In this study, measurement instruments on a mobile cart were used to identify spatial and time variation of nanoparticle migration [Evans *et al.*, 2010].

The face velocity and flow rate of the enclosure and the local exhaust ventilation were measured with a thermal anemometer to compare with existing standards specified by OSHA and ACGIH. For the ventilated enclosure, measurements were taken in the direction perpendicular to the plane of the opening and at the center of each equal area. Therefore, there were 9 measurements when the enclosure door was fully open and 3 measurements when the door was partially open. The tasks performed in the production areas were monitored by direct-reading instruments to determine the real-time contribution of specific operations for nanoparticle emissions [Brouwer *et al.*, 2004; Peters *et al.*, 2009].

## Sampling Plan

An initial meeting was held on May 10, 2010, to talk with the company management and discuss the site survey to evaluate the existing engineering controls. A short walk-through survey was conducted after the meeting to observe the tasks. Some tasks were identified without proper controls that could potentially release nanoparticles into the workplace. For quantitatively identifying the critical steps in the production areas, direct-reading instruments were used to monitor the manufacturing processes and the operation of the compressor. Area monitoring was done with the same instruments in the production areas and the non-production areas (laboratories and offices) to examine particle distributions in the facility.

Direct-reading instruments used in real-time mode can help identify major emission sources to assess the efficiency of control measures in the nanomanufacturing workplace. They provide continuous measurements of concentrations that can be correlated with the specific production equipment and work processes. Because of the lack of established exposure criteria, measurements of number, size, mass, and surface area concentrations of nanomaterials are needed [Mark, 2007]. The instruments used to measure particle concentrations in this survey were the Fast Mobility Particle Sizer (FMPS) spectrometer, Aerodynamic Particle Sizer (APS) spectrometer, DustTrak aerosol monitor, and Miniature Black Carbon monitor.

An FMPS (Model 3091, TSI Inc.) was used to identify particle emissions in this in-depth site study. The FMPS uses a corona charger to positively charge particles and simultaneously determines number size distributions with an array of electrometers. It is capable of measuring particle sizes ranging from 5.6 to 560 nm in a time of resolution of 1 second. Real-time measurement is usually required to quickly determine fluctuations of size/number distributions of released nanoparticles in the nanomanufacturing workplace. The FMPS has been used in field studies for exposure assessment [Bello *et al.*, 2009; Tsai *et al.*, 2009].

Aged nanoparticles, originally released from any large-scale nanoparticle manufacturing process, tend to agglomerate to become larger sized particle clusters. Using a light-scattering technique, an APS (Model 3022, TSI Inc.) was used at this study site to measure aerodynamic diameters of larger particles in the range of 0.5 to 20  $\mu\text{m}$ . Like the FMPS, the sampling frequency of the APS can be as short as 1 sec. Therefore, the measurement results from the APS and FMPS can provide a full spectrum of airborne particle size and number distributions in work areas.

Mass concentration is traditionally used as a metric for exposure assessment. A real-time laser photometer, the DustTrak DRX aerosol monitor (Model 8533, TSI Inc.), was used to measure mass concentrations of contaminants for this survey. It can measure particles ranging from 0.1 to 10  $\mu\text{m}$  at concentrations between 0.001 and 150  $\text{mg}/\text{m}^3$  and can display mass fractions in the modes of  $\text{PM}_{10}$ ,  $\text{PM}_{2.5}$ ,  $\text{PM}_{10}$  (respirable particulate matter), and total mass concentration. Studies have shown that the measurement results from a DustTrak were comparable to the data from filter-based gravimetric sampling method and Tapered Element Oscillating Microbalance (TEOM, an EPA standard reference equivalent method) [Lehocky & Williams, 1996; Kim *et al.*, 2004; TSI Inc., 2008].

The Miniature Black Carbon (BC) monitor (Model AE51, TSI Inc.) was used to measure carbonaceous particles by analyzing air samples with its built-in Teflon coated borosilicate glass fiber media. Unfortunately, the BC monitor showed higher noise on many measurement points (i.e., negative values), when it sampled every second. The mass-based concentration data for carbonaceous particles were collected for reference only because the BC monitor was operated at a 1-minute sampling time interval.

The three real-time direct-reading instruments (FMPS, APS, and DustTrak), the BC monitor, and a laptop computer were integrated on a mobile sampling cart to facilitate data collection during the field survey (**Figure 6**). In addition to collecting particle concentration data, face velocities for the enclosure and fume hoods, and flow rates at the local exhaust and wall fan were measured using an air velocity meter (VelociCalc Plus hot wire anemometer, Model 8386, TSI Inc.) with a telescoping probe.

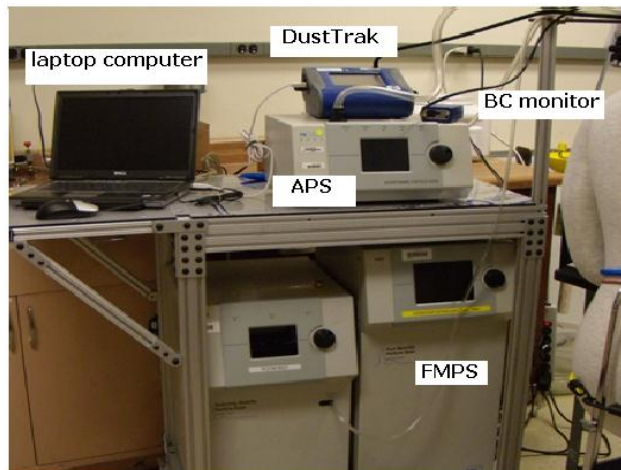


**Figure 6:** Mobile sampling cart to transport sampling instruments during the survey.

A test of changing the tube cooling time was done to evaluate whether process modification can reduce emissions. Three glass tubes were prepared as usual, but the insulators were removed after different cooling times (**Figure 7**). The insulators on the third tube were removed as soon as the tube completed the post-treatment in the reactor. The second tube was cooled for a longer time before removing the insulators; the first tube spent the longest cooling time before removing the insulators. Therefore, there are three different tube temperatures: hot for the third tube, warm for the second tube, and cold for the first tube.

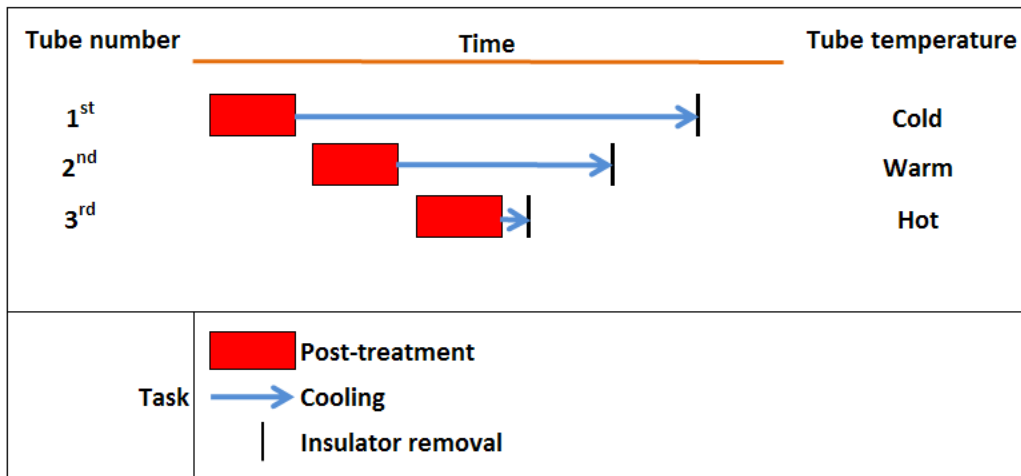


**Figure 7:** Test plan to check how the tube cooling time changes nanomaterial emissions during product harvesting in the post-treatment process.

## Results and Discussion

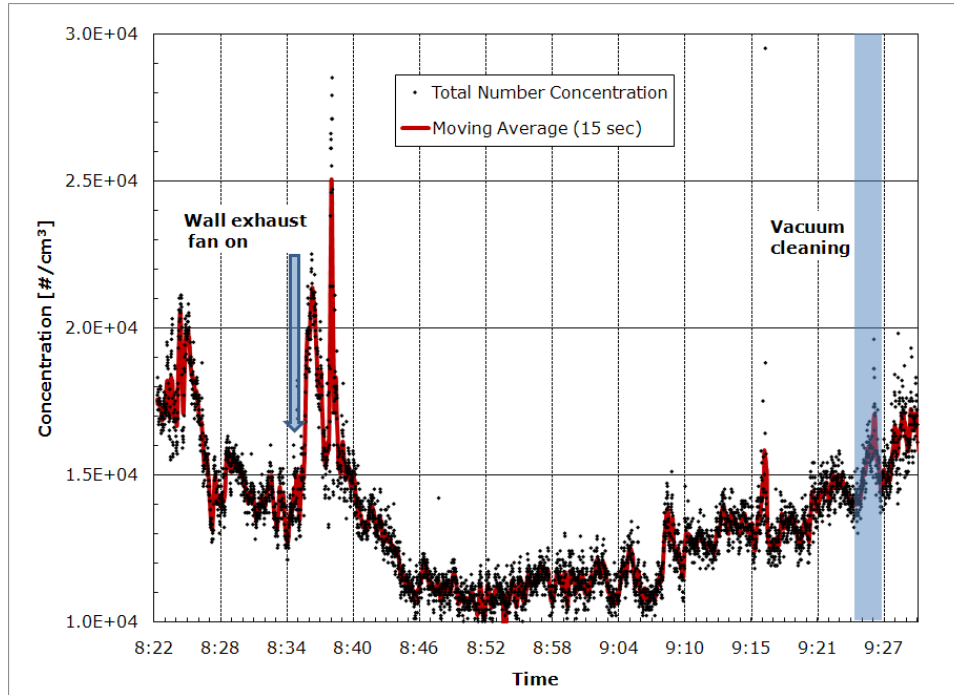
### Concentration Measurements of Area Samples

The concentrations of area samples were measured at Location AM1 (**Figure 1**) outside the refining area on September 29, 2010, from 10:03 to 10:33. There was no intensive activity around Location AM1, and stable concentration trends were recorded by the instruments (**Figure A-1**). On September 30, 2010, Location AM2 near the post-treatment area was monitored from 08:22 to 09:30. During this area monitoring, workers were performing the preparation activities for the post-treatment process. The area concentrations were influenced by some activities such as starting the wall exhaust fan and cleaning the workplace with a vacuum (**Figure 8**). The wall fan appeared to double the total fine particle numbers (**Figure 8-a** for FMPS results) and the operation of the vacuum contributed an increase of total particle mass by one order of magnitude (**Figure 8-b** for DustTrak results). However, no major changes were found from the APS, suggesting that these activities did not generate large size particles.

The particle size distributions at this facility were substantially similar (**Figure 9** for FMPS results for area monitoring). They can be presented by the average size distribution that was polydisperse with maxima at 10, 20, and 70 nm. Stable area concentrations were also found with the APS for large particles and the DustTrak for total particle mass.

On the basis of area monitoring in the production areas, the overall averages of total number concentration were  $\sim 15,000$  particles per cubic centimeter ( $\#/cm^3$ ) for particles below 560 nm (according to the FMPS) and  $\sim 42 \#/cm^3$  for particles larger than  $0.5 \mu m$  (according to the APS). The mass concentration from the DustTrak was  $\sim 0.025 \text{ mg}/m^3$ .

(a)



(b)

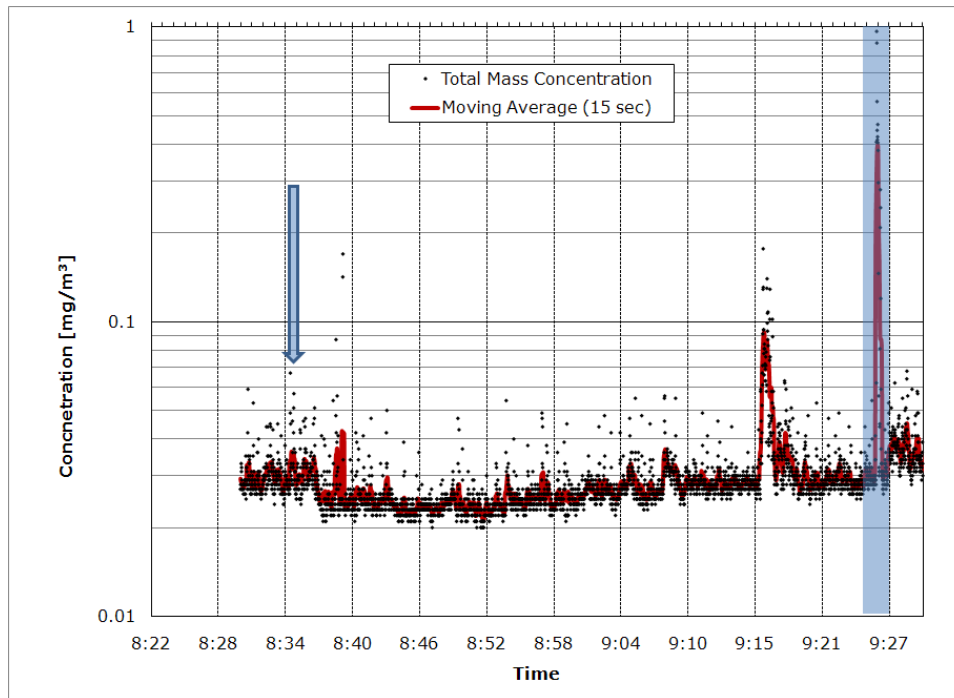


**Figure 8:** Area monitoring data as measured by (a) FMPS and (b) DustTrak in Location AM2 on 09/30/10.

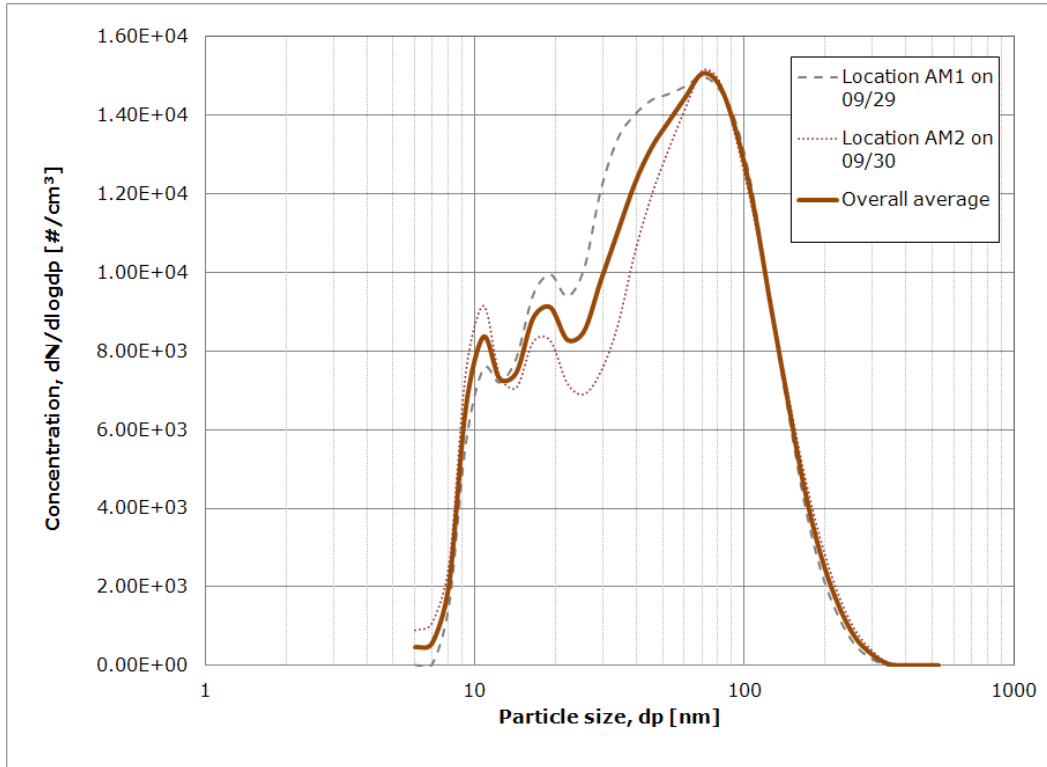


**Figure 9:** Average particle size distributions monitored by the FMPS during area monitoring at Locations AM1 and AM2 shown in **Figure 1**.

### Examination of Airflow around Enclosure and Local Exhaust

A thermal anemometer was used to check the face velocities on the enclosure opening in the refining area. The opening of the enclosure is 2 ft by 2 ft when fully opened, but the height of the opening is less than 1 ft when the enclosure is fully lowered. Therefore, the enclosure is usually operated with the door fully open to perform tasks easily. A 1 ft by 1 ft imaginary grid pattern is required to equally divide the hood opening into vertical and horizontal dimensions, and velocity readings should be taken with the anemometer at the center of the grid spaces [ANSI/ASHRAE 110-1995 Standard, 1995]. To obtain more accurate data in this survey, face velocity measurements were taken from nine grid spaces for the enclosure door raised and three grid spaces for the door lowered. Measurements over a period of 1 minute were collected at each point. The overall average face velocity of this enclosure was 78 fpm when the enclosure door was open and 182 fpm when the door was lowered (**Table 1**). Similar measurements taken

from the fume hoods located in the Lab 1 room (**Figure 1**) indicated that the fume hoods were operated at a lower average face velocity of 54 fpm for R&D activities.

**Table 1:** Face velocity measurements for the ventilated enclosure and fume hood.

Location	Ventilated Enclosure in the refining area						Fume hood in the Lab 1 room		
Date	09/29/10						09/30/10		
Enclosure door	Door raised			Door lowered			Door lowered		
Measurement grid size	$\frac{2}{3}'' \times \frac{2}{3}''$			$\frac{2}{3}'' \times \frac{2}{3}''$			1'' x 1''		
Average velocity at the center of the grid space [fpm]	96	96	73	X	X	X	X	X	X
	68	84	58	X	X	X	X	X	X
	80	93	56	176	192	178	54	56	53
Overall average face velocity [fpm]	78			182			54		

The air volume flow rate of the wall fan installed in the post-treatment area was estimated from anemometer measurements made on 12 grid spaces (**Table 2**). A local exhaust control on the top of the reactor was the only control measure used to mitigate nanomaterial emissions during the post-treatment process. The local exhaust was a 4'' diameter flexible duct operated at an average face velocity of 1105 fpm (96 cfm). The local exhaust was simply inserted into the exhaust duct (12'' diameter) of one of the canopy hoods (**Figure 5**). The anemometer measurements showed that the exhaust duct was operated at an average velocity of 1363 fpm, and an estimated flow rate of 1070 cfm.

**Table 2:** Estimated air volume flow rate of the wall fan (4.5 ft x 4.25 ft).

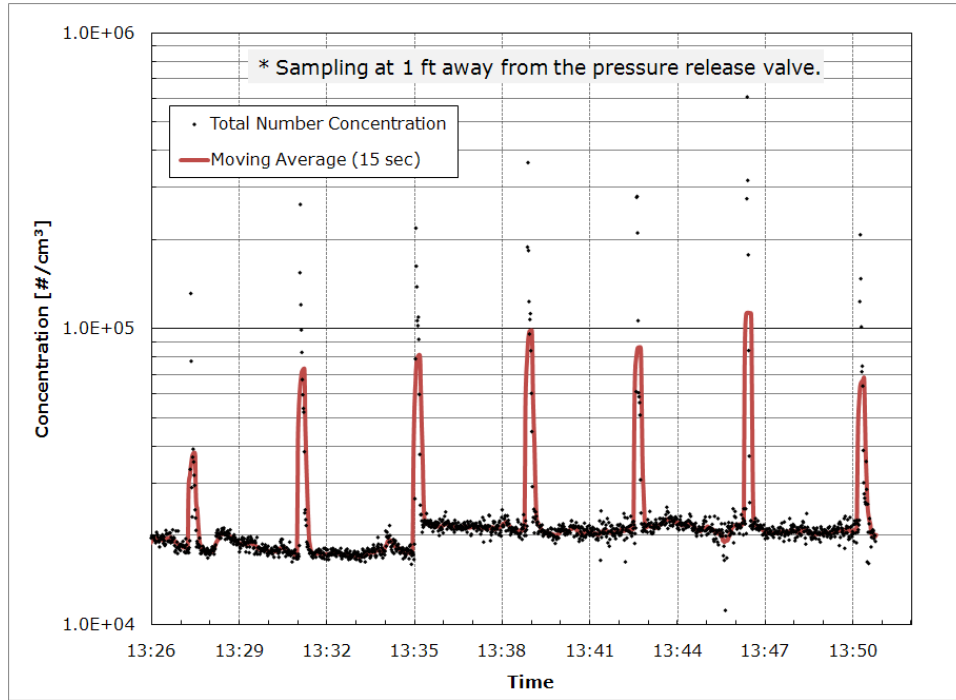
Date	09/29/10			09/30/10		
Measurement grid size	~ 1" x 1"					
Average velocity at the center of the grid space [fpm]	251	286	490	540	283	525
	630	258	720	710	240	685
	820	273	740	700	230	910
	550	204	605	810	244	670
Mean air velocity [fpm]	486			546		
Overall air velocity [fpm]	516					
Total flow rate [cfm]	9861					

### Compressor

The compressor near the refining area released high pressure air to the workplace nearly every 4 minutes to remove moisture from the air tank. Measurement data showed that a large quantity of nanoparticles  $\sim 10$  nm (approximately  $4 \times 10^4 \sim 1 \times 10^6$  #/cm<sup>3</sup>) was found while the air was released from the pressure valve on the compressor (**Figure 10**), but not many large particles  $>0.1$   $\mu\text{m}$  were found from the APS and DustTrak (**Figure A-2** and **Figure A-3**). The background data were collected from 11:35 to 13:00 on September 30, 2010. The sampling locations were changed to verify the concentrations of small particles being released from the compressor (**Figure 10**). At the pressure release valve, the total number concentration was  $\sim 300,000$  #/cm<sup>3</sup> on average, approximately 30 times higher than the background average ( $\sim 10,300$  #/cm<sup>3</sup>). The total number concentration was  $\sim 80,000$  #/cm<sup>3</sup> at one foot from the release point, and  $\sim 40,000$  #/cm<sup>3</sup> at 3 feet away from the release point.

The average size distributions of particles at different locations are presented in **Figure 11** to illustrate the evolution of particles released from the compressor into the workplace. The compressor released nanoparticles at 10 nm, approximately 50 times higher than the background. As shown in the data sampling at 3 ft away from the release valve, the quantity of those nanoparticles fell dramatically once they were dispersed in the workplace. A mist emitted by the compressor generated nanosized particles of air rather than engineered nanomaterials. It was a stable source of these nanoparticles.

(a)



(b)

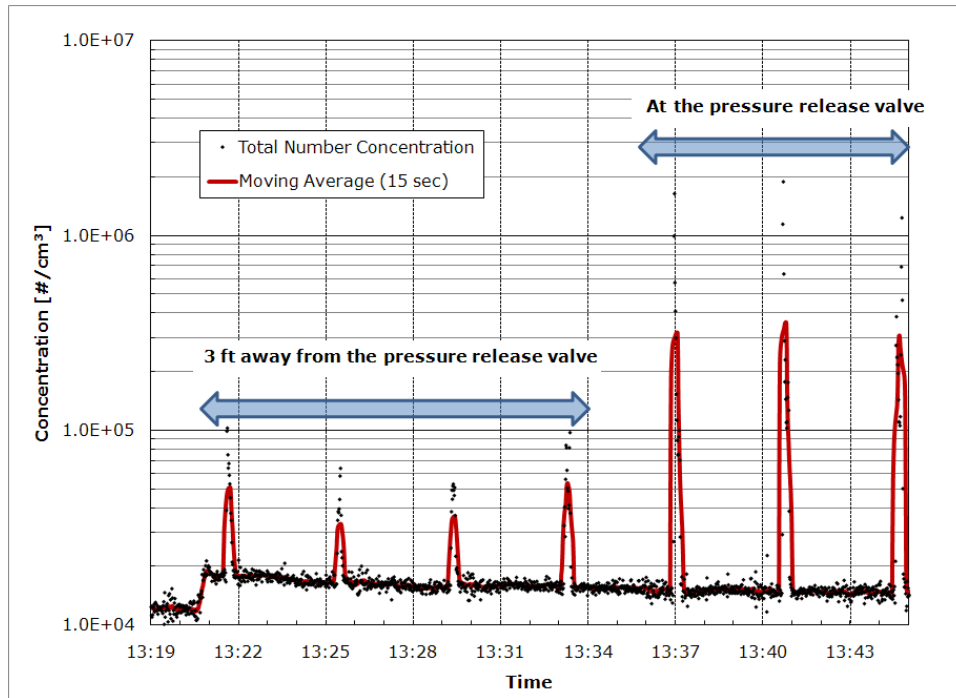


**Figure 10:** Sampling results from the compressor near the refining area as measured by FMPS on (a) on 09/29/10 and (b) on 09/30/10.

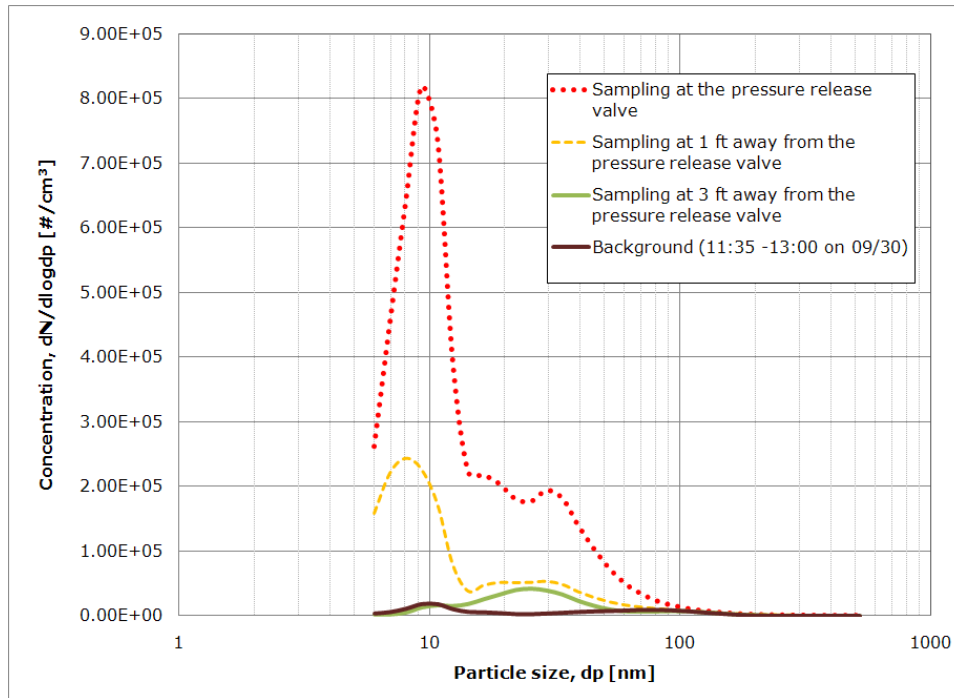


**Figure 11:** Average size distributions of particles released from the compressor as measured by the FMPS. The overall average data from area monitoring presented in **Figure 9** are shown here for comparison.

## Refining Process

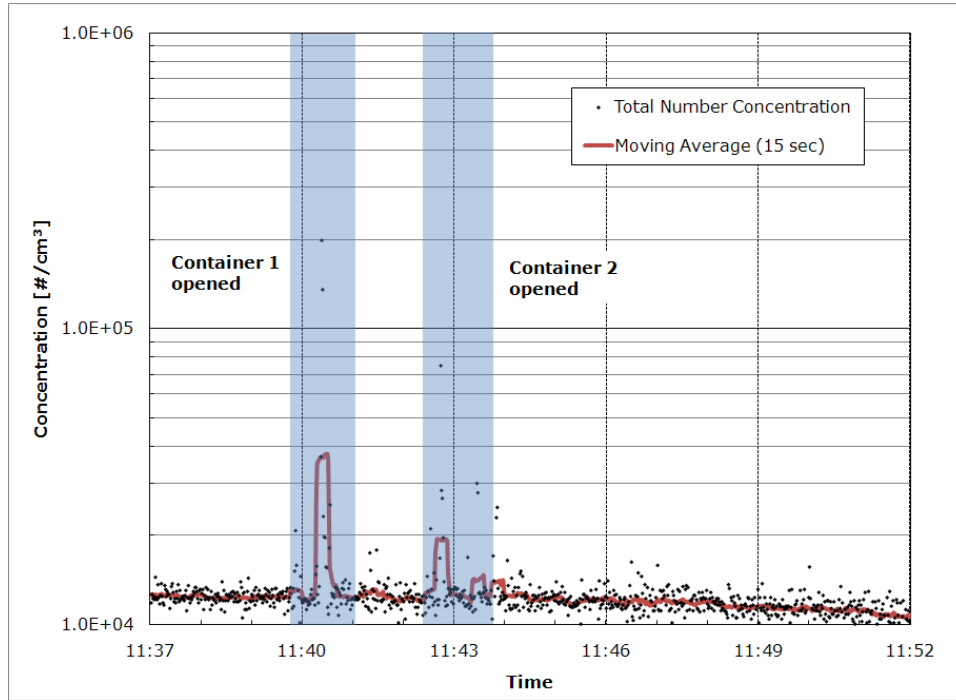
Direct-reading instruments were used to monitor all the steps in the refining area. Because of the lack of proper controls, the data indicated that the tasks starting from raw material preparation to product harvesting released agglomerates or nanoparticles to the workplace. It was also found that nanomaterials escaped from a ventilated enclosure when product transfer was performed inside this control measure.

## Product Harvesting

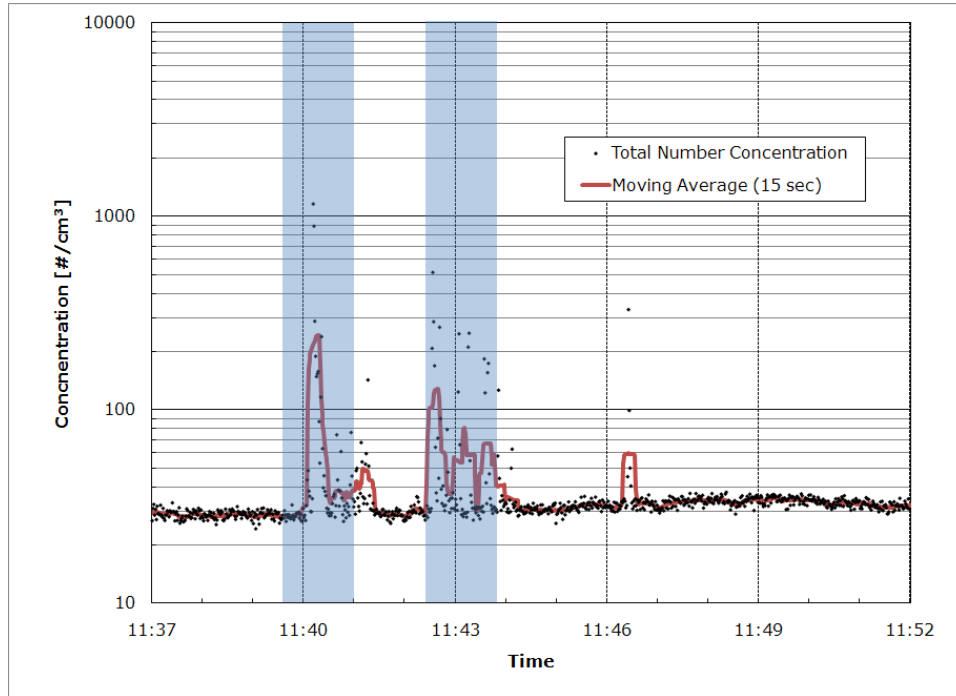
The harvesting processes from process tanks were examined to understand if the tasks released nanomaterials, because no specific control measures were used in place. Two tests were done on September 29, 2010. The first test, monitoring the product harvesting from Process Tank 1 only, was done from 11:37 to 11:52. The second test, monitoring the product harvesting from both tanks and the tasks performed in the ventilated enclosure, was done from 16:25 to 16:40.

The FMPS easily identified nanomaterial emissions while the operator opened containers to harvest products from Process Tank 1 (**Figure 12-a**). The concentration of fine particles released from Container 1 rose nearly three times higher than the background level ( $\sim 12,000 \text{ \#/cm}^3$ , monitored by the FMPS from 10:36 to 10:46). However, the APS used to detect larger size particles ( $>0.5 \text{ \mu m}$ ) showed stronger signals (**Figure 12-b**) compared to the results from the FMPS. The peak concentration of large particles in this harvesting location was nearly 20 times higher than the average background concentration ( $\sim 43 \text{ \#/cm}^3$ ). The summary results from the DustTrak (**Figure 12-c**) and the BC monitor (**Figure 12-d**) were consistent with the data provided by the APS. Moreover, the mass concentrations increased almost two orders of magnitude while opening the containers. In other words, larger size particles  $>0.5 \text{ \mu m}$  (or agglomerated nanomaterials) were released into the workplace when containers were opened to harvest products.

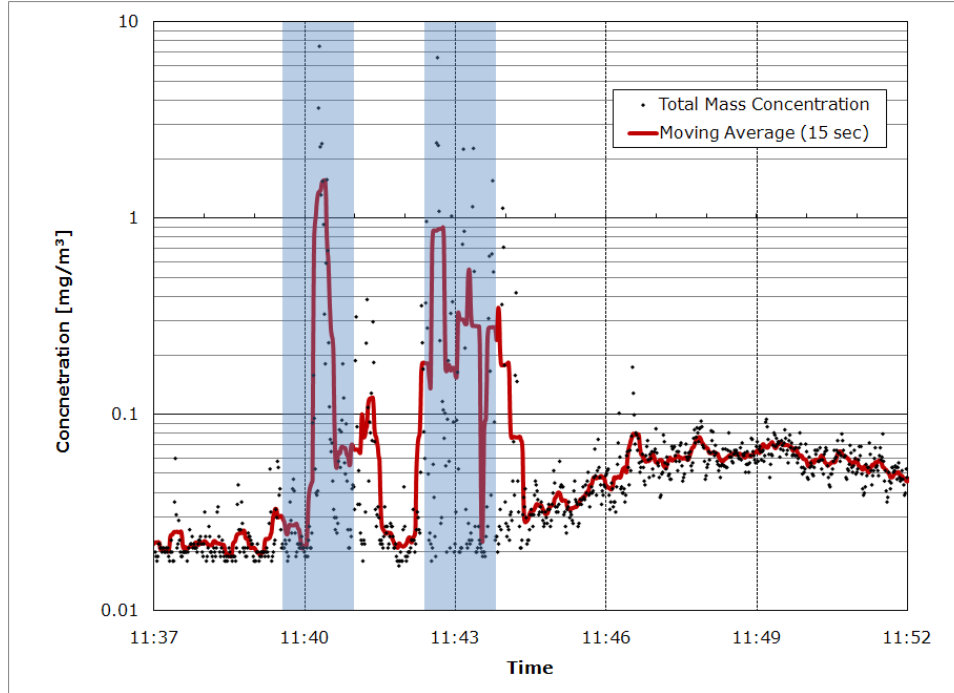
(a)



(b)



(c)



(d)

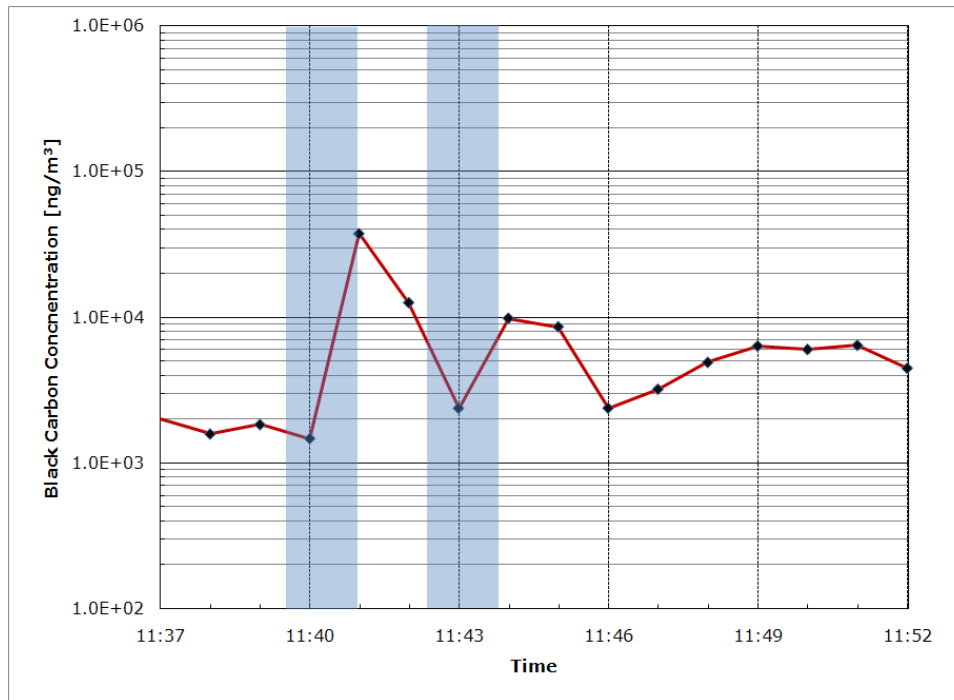
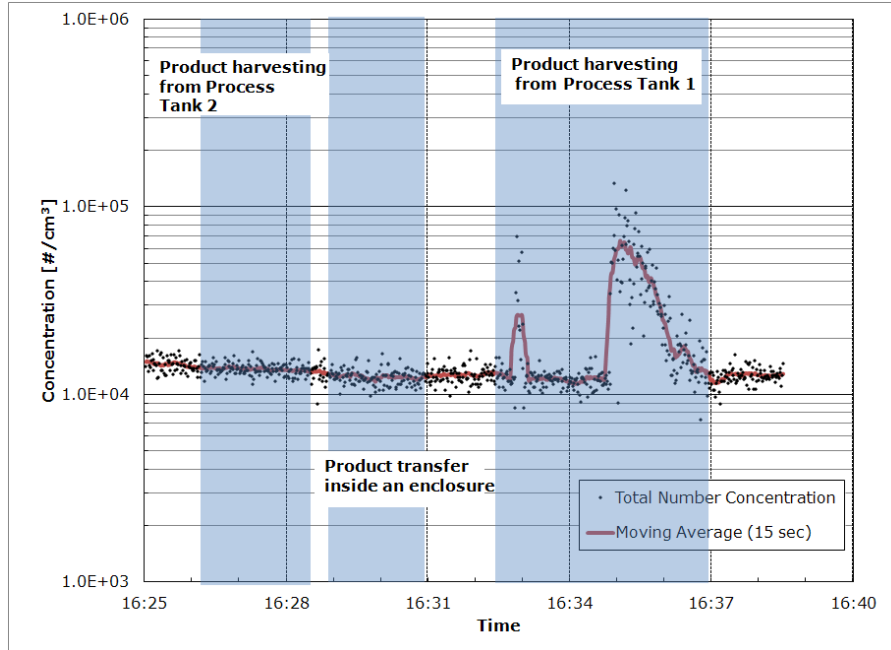


**Figure 12:** Sampling results from Process Tank 1 during product harvesting as measured by the (a) FMPS, (b) APS, (c) DustTrak and (d) BC monitor on 09/29/10.

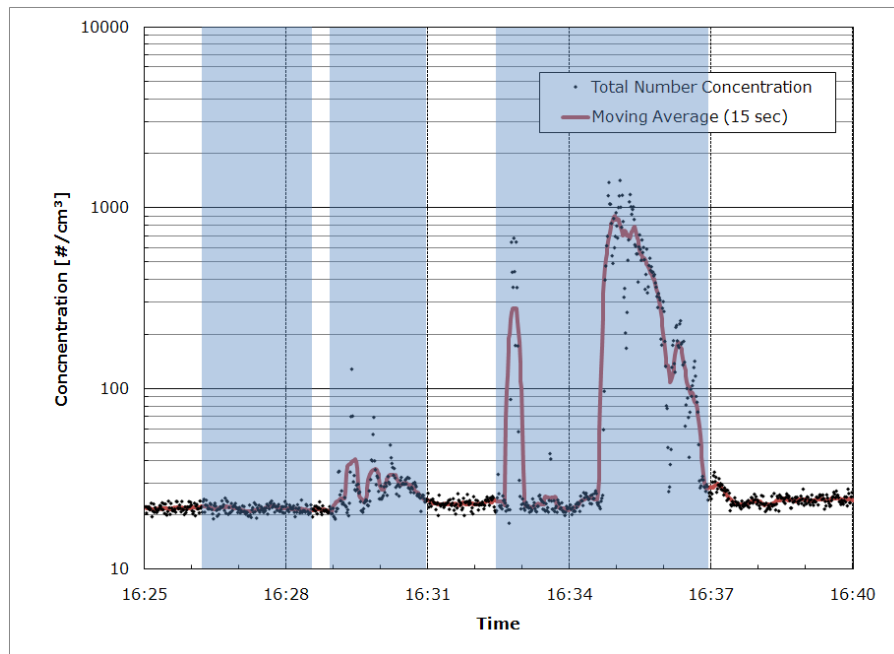
The second test was conducted while harvesting from both process tanks and during product transfer and packaging inside the ventilated enclosure. The FMPS detected no noticeable change in particle concentration during harvesting from Process Tank 2, but Process Tank 1 released particles during product harvesting (**Figure 13-a**). Product transferring and packaging performed inside the enclosure produced no noticeable emission of small particles. The APS data in **Figure 13-b** showed that opening containers to harvest products from process Tank 1 released larger size particles, but Process Tank 2 did not. **Figure 13-b** also showed that some large size particles escaped from the enclosure during transferring and packing of the products. Note that the sampling ports were located at the breathing zone of the operator working on the tasks inside the enclosure. The data from the DustTrak (**Figure 13-c**) and the BC monitor (**Figure 13-d**) showed similar results as the APS.

The size distribution results from the FMPS and APS when monitoring product harvesting from Production Area 1 are presented in **Figure 14**. The background data from the same instruments are displayed as well for comparison. The FMPS data (**Figure 14-a**) indicated that the size distributions had peak concentrations at less than 10 nm (close to the detection limit of the FMPS) and at approximately 100 nm. The APS data (**Figure 14-b**) showed a peak at 2  $\mu\text{m}$ . It appears that opening the containers to harvest products could result in emissions of agglomerated nanomaterials. For the transfer of nanomaterials inside the ventilated enclosure, fugitive particles were concentrated at 30 nm and 3  $\mu\text{m}$  according to the size distribution analysis from the FMPS and APS (**Figure 14-a** and **Figure 14-b**). The particle number and mass concentrations generated from the tasks performed in the enclosure were nearly two orders of magnitude lower than those from harvesting without appropriate control measures.

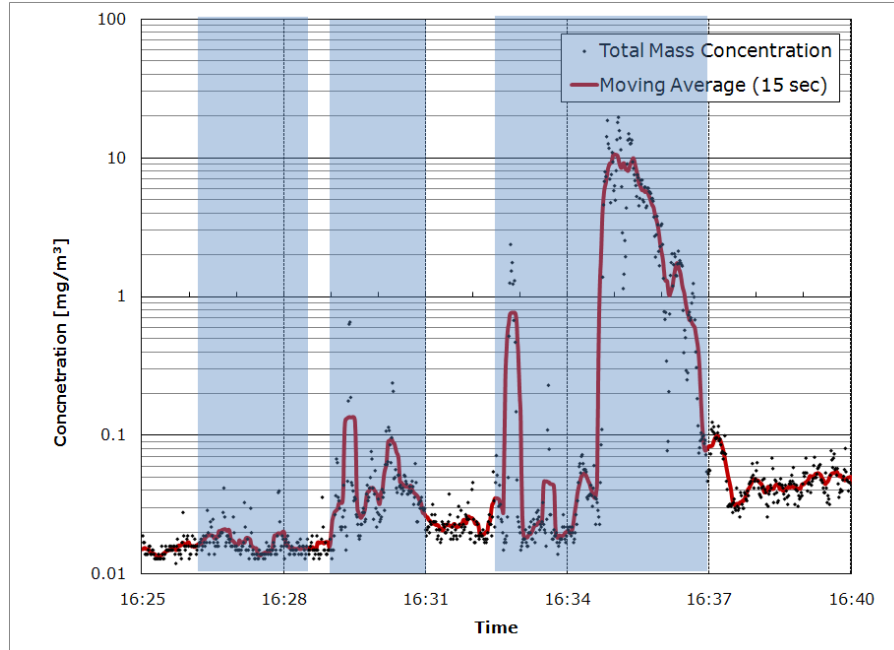
(a)



(b)



(c)



(d)

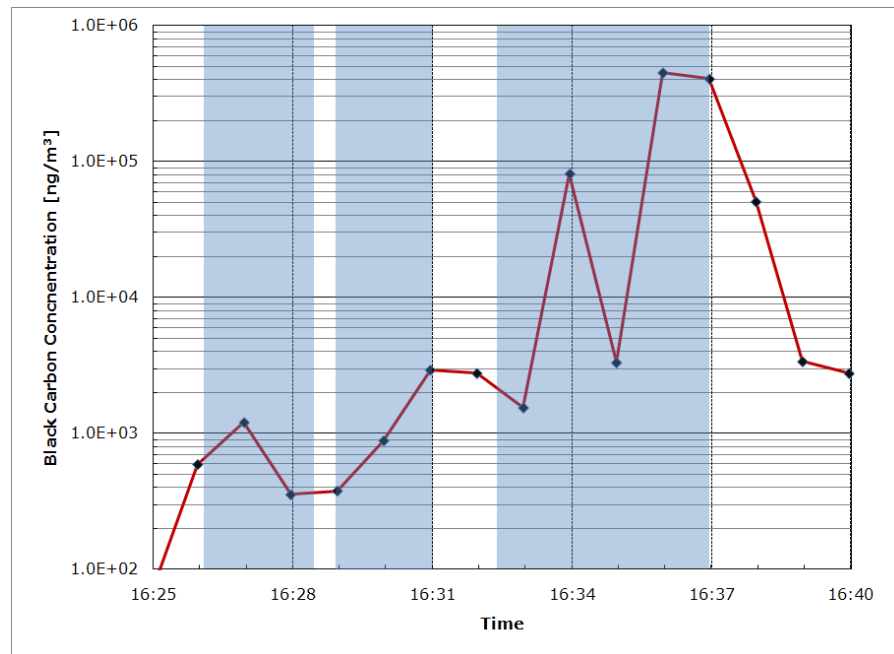
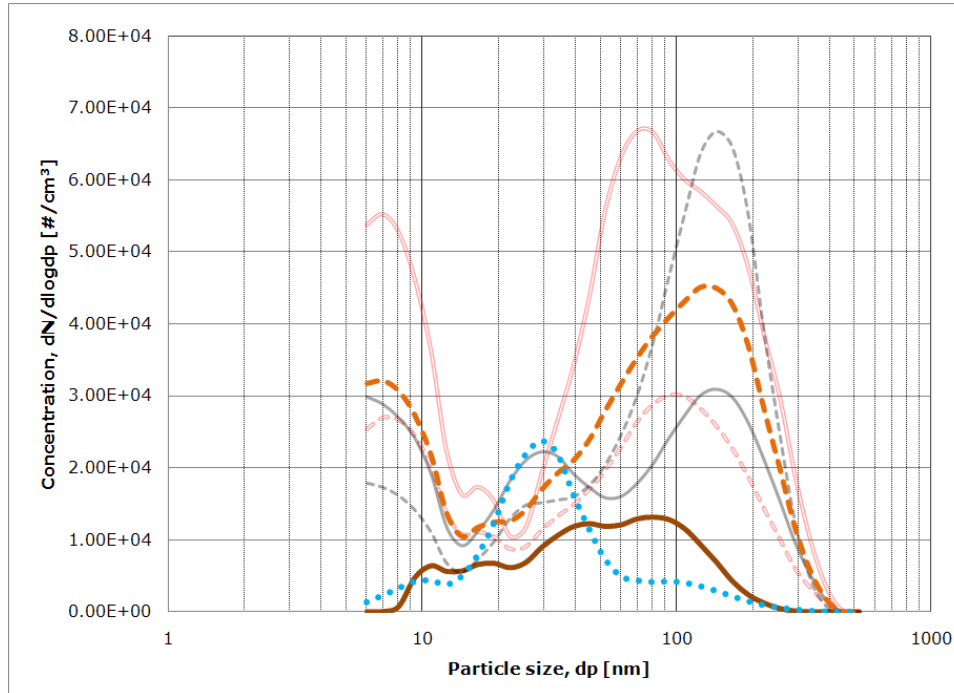


**Figure 13:** Sampling results from both process tanks during product harvesting and product transfer inside the enclosure as measured by (a) FMPS, (b) APS, (c) DustTrak, and (d) BC monitor on 09/29/10. Note that the sampling ports were located near the breathing zone of the operator while the operator transferred products inside the enclosure.

(a)



(b)

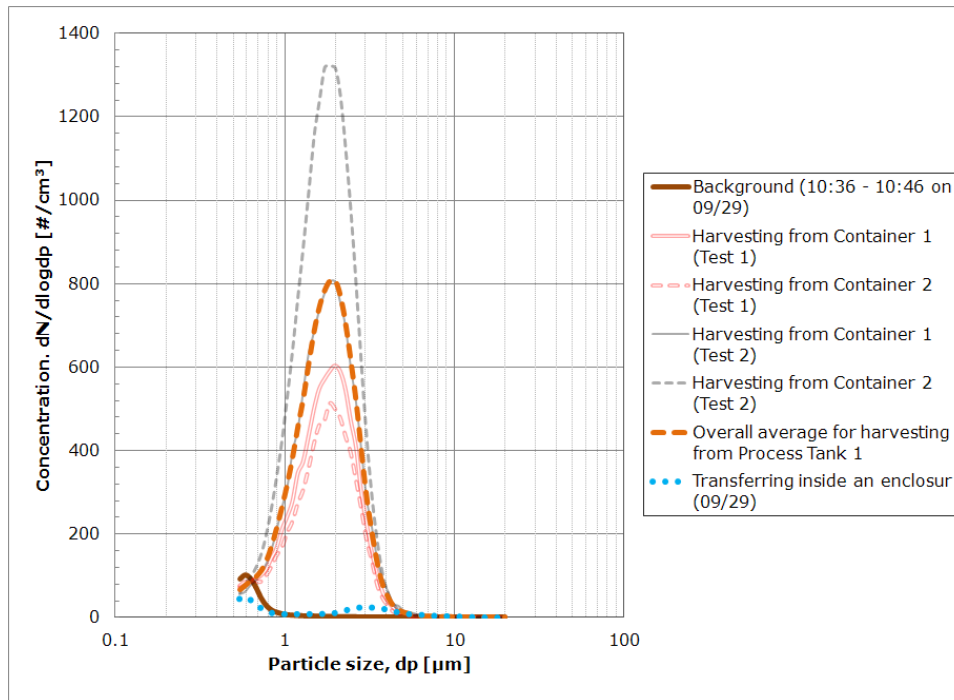


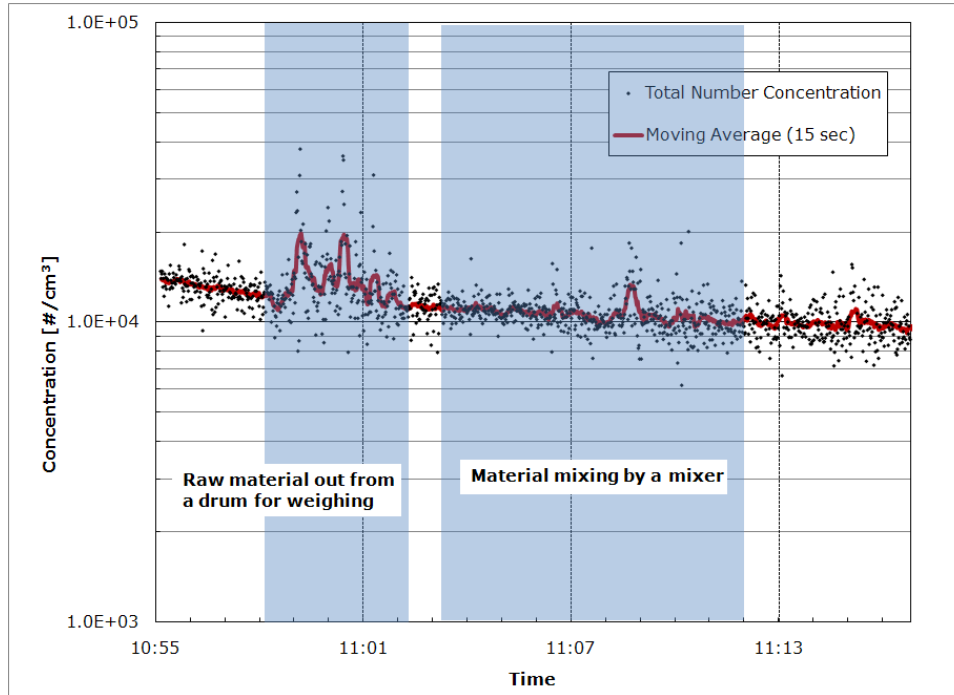
**Figure 14:** Size distributions from (a) FMPS and (b) APS based on the measurement data from **Figure 12** (Test 1) and **Figure 13** (Test 2).

## Raw Material Preparation

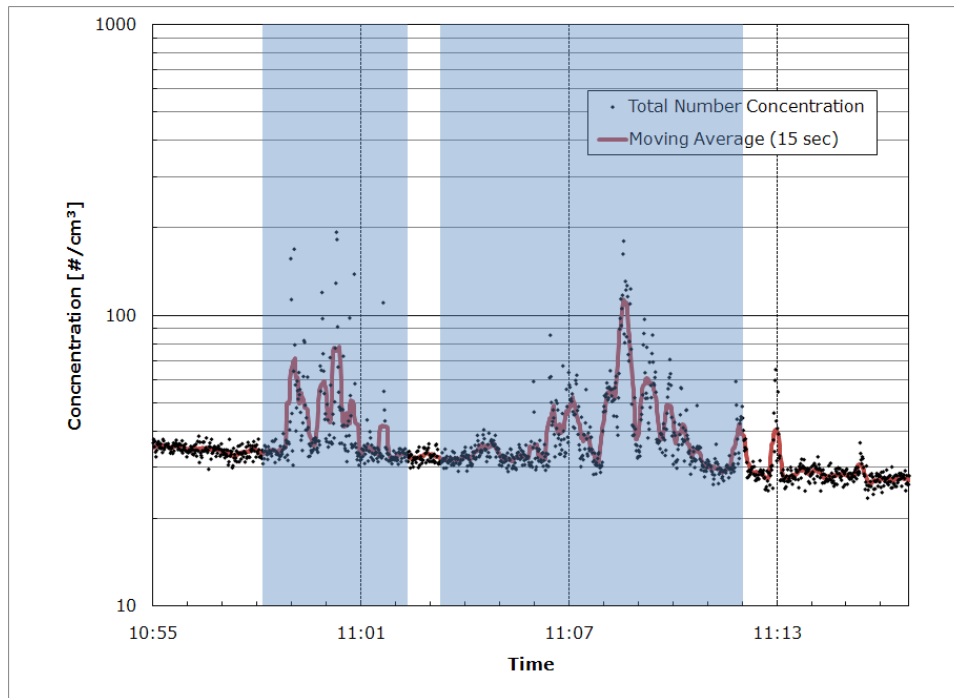
On 09/30/10, the procedures for preparing raw materials in the refining area were studied, because dry powders were handled by workers without using any engineering controls.

The FMPS did not show a dramatic increase in emissions of small size particles during raw material preparation (**Figure 15-a**), but the APS data gave a clearer view of large particles released from raw material transfer and mixing (**Figure 15-b**). The mass concentrations from the DustTrak measurement (**Figure 15-c**) and the black carbon concentrations from the BC monitor (**Figure 15-d**) presented stronger evidence that raw materials were emitted during these tasks. Size distributions from the APS were summarized in **Figure 16** to show changes in particle size during raw material preparation. Compared with background, the task of removing raw materials out from the drum released agglomerates at 3  $\mu\text{m}$ , while the mixing process produced finer particles at  $\sim 1.6 \mu\text{m}$ .

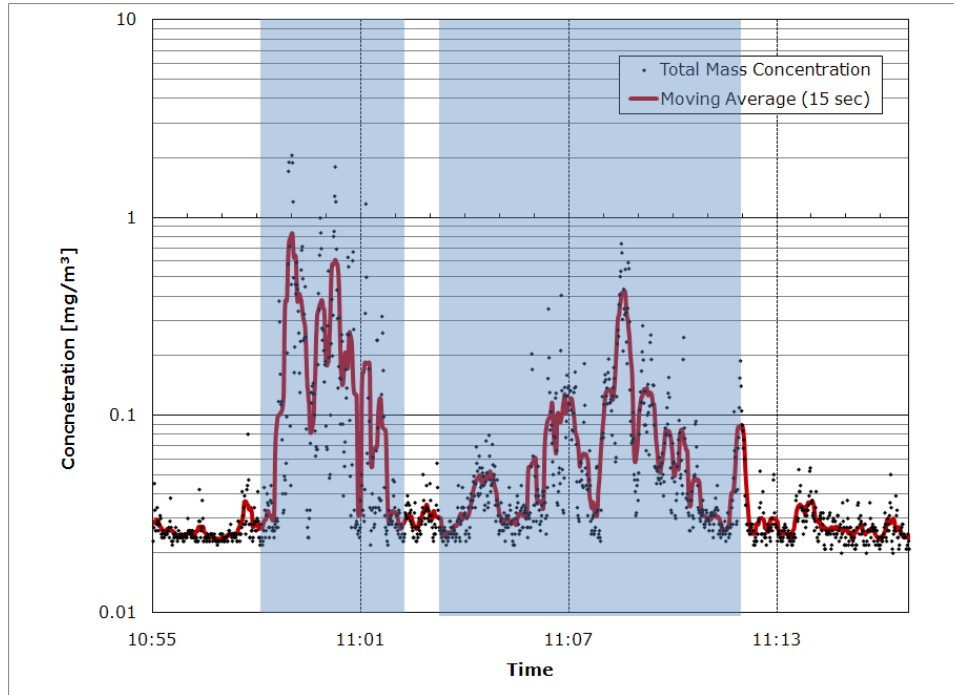
(a)



(b)



(c)



(d)

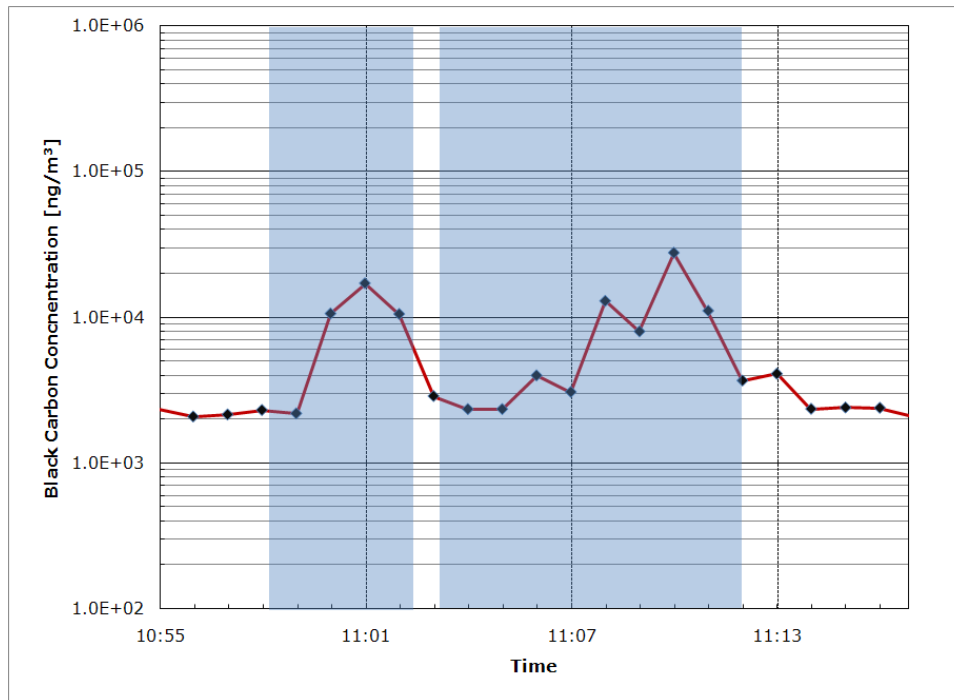


**Figure 15:** Sampling results from raw material preparation for the refining process as measured by (a) FMPS, (b) APS, (c) DustTrak, and (d) BC monitor on 09/30/10.

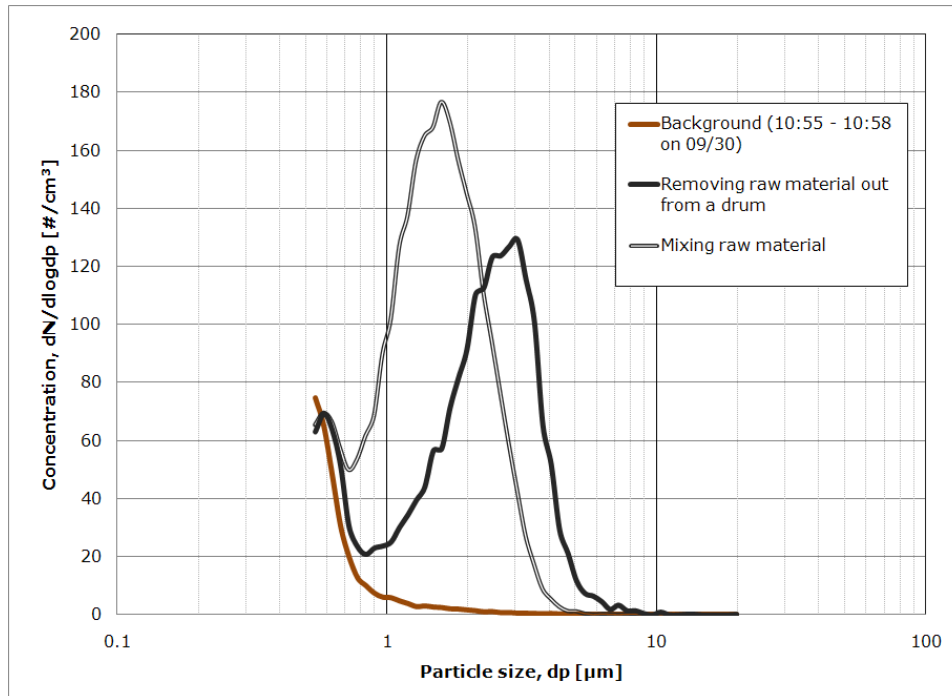


**Figure 16:** Size analysis for raw material preparation for the refining process as measured by APS on 09/30/10.

### Post-Treatment Process

To identify nanomaterial emissions, the whole process was monitored, starting with material preparation, material treatment, tube cooling, insulator removal, product harvesting, and finally workplace cleaning. The instrument sampling ports were close to the anticipated sources to characterize the variation of particle concentrations in every step. The real-time air monitoring data obtained from the FMPS for tube cooling and product harvesting were reported in this section. The APS, DustTrak, and BC monitor did not show appreciable variation when monitoring these two steps. For other steps, all the direct-reading instruments showed no appreciable change in particle concentrations.

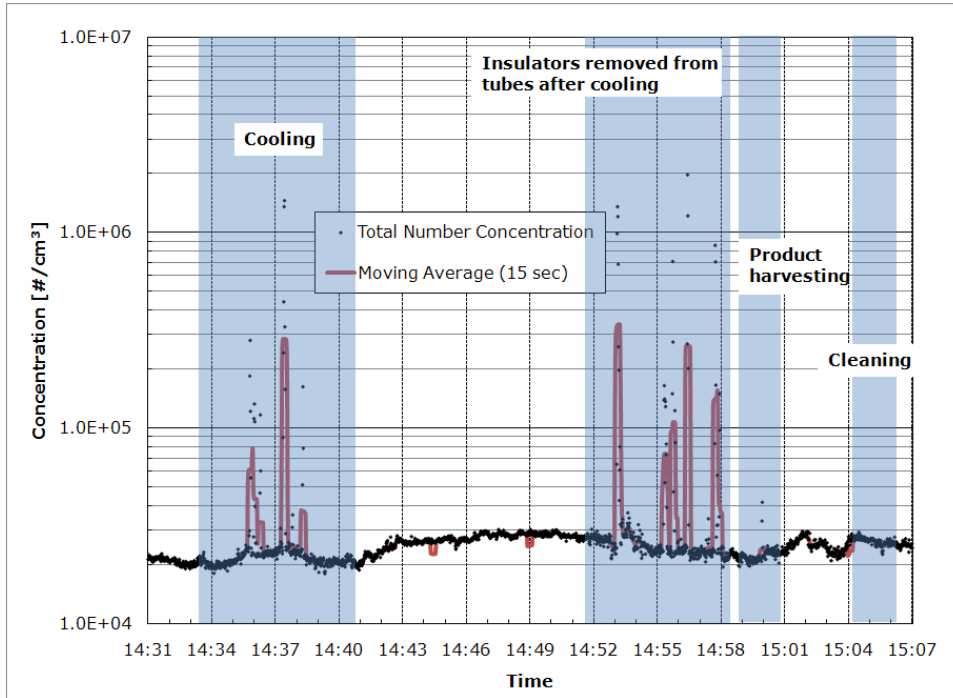
## Tube Cooling and Insulator Removal

Monitoring the post-treatment process was performed twice on September 29, 2010. Major particle releases were found during the steps of tube cooling and removal of insulators from tubes as monitored by the FMPS (**Figure 17**). No meaningful variation was found with the APS and DustTrak (**Figure A-4** and **Figure A-5**) except that large particles were detected occasionally during insulator removal. The results indicated that both steps released very fine particles at peak concentrations nearly two orders of magnitude greater than the average background concentration ( $\sim 2 \times 10^4 \text{ \#/cm}^3$ ). The local exhaust system did not provide adequate ventilation for mitigating nanoparticle emissions.

Sharp peaks in number concentrations as measured by the FMPS during tube cooling all came from the third tube. However, particle release was identified from every tube once the insulators were removed for product harvesting. Product harvesting from the tubes did not produce measurable particle variations noted by the measuring instruments.

Examining the size distributions reveals the variation of nanoparticles released from the process. Tube cooling released a large quantity of nanoparticles whose peak concentrations can be over  $2 \times 10^6 \text{ \#/cm}^3$  (**Figure 17**), and most of them were less than 15 nm (**Figure 18**). Similar size distribution analysis was performed for the insulator removal step from the tubes, summarized in **Figure 19**. Comparison between **Figure 18** and **Figure 19** showed that nanoparticles released during insulator removal are similar to those released during tube cooling, less than 15 nm. Though the cooling time was long enough to cool down the temperature of tubes, insulator removal still produced different levels of particle concentrations from the tubes (**Figure 17** and **Figure 19**).

(a)



(b)

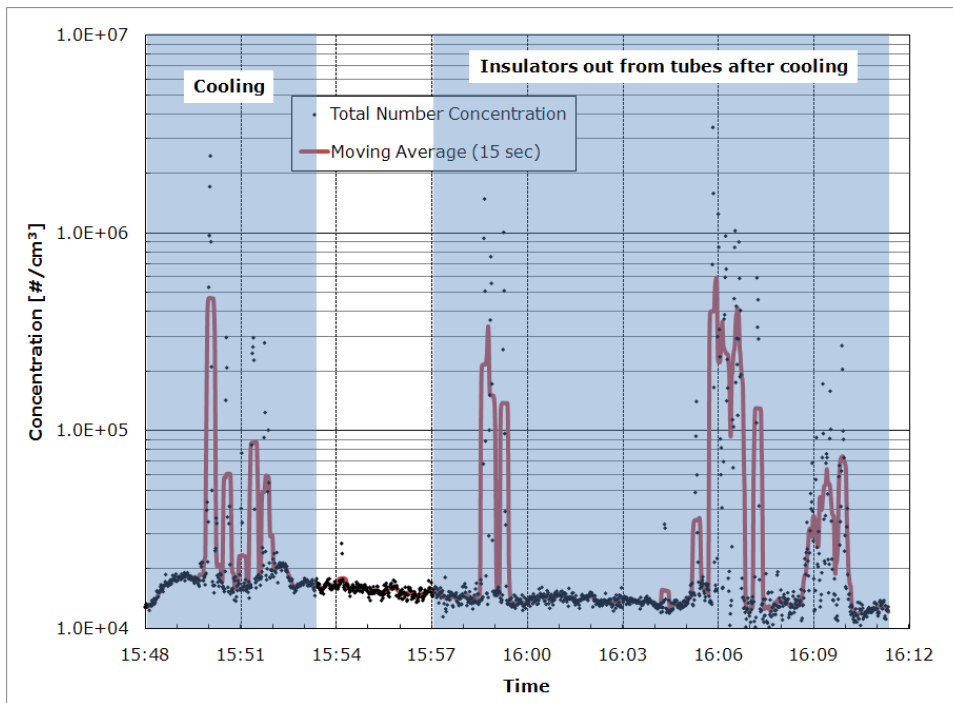


**Figure 17:** Sampling results of (a) Test 1 and (b) Test 2 from the post-treatment process as monitored by FMPS on 09/29/10. The third tube was the only one to release particles during tube cooling.

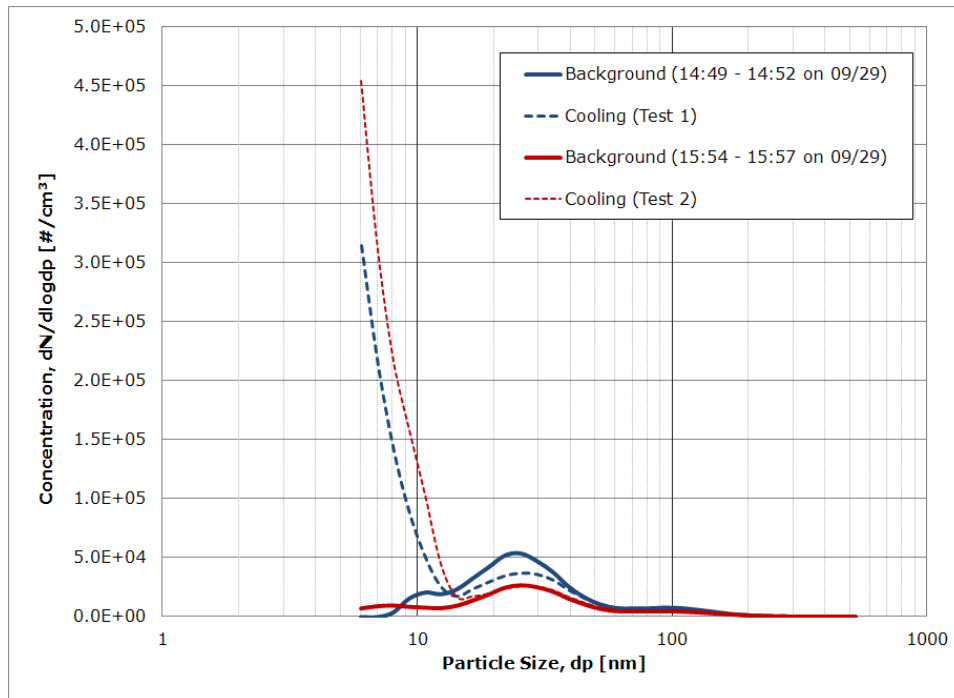
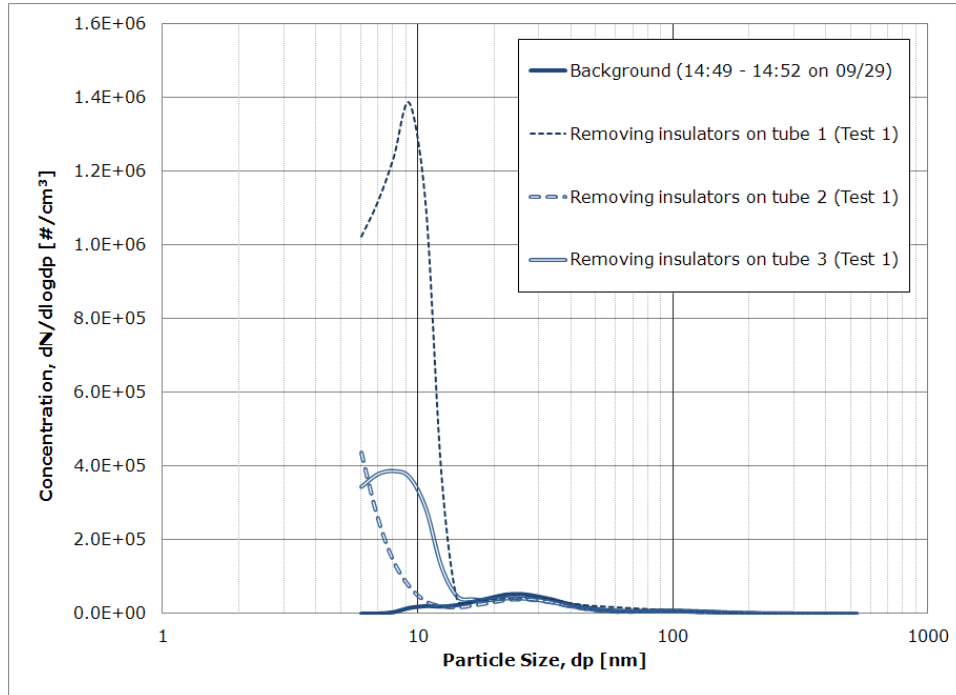


**Figure 18:** Size distribution analysis for particle release from tube cooling presented in **Figure 17**.

(a)



(b)

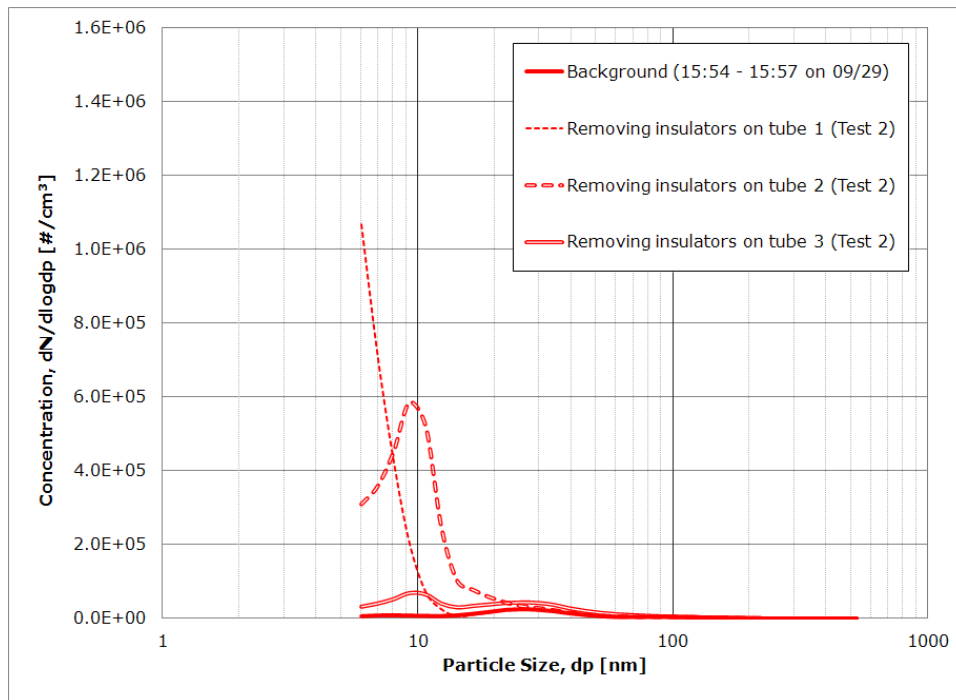


**Figure 19:** Size distribution analysis for the step of insulator removal from the tubes for following product harvesting in (a) Test 1 and (b) Test 2 as presented in **Figure 17**.

## Effect of Tube Cooling Time

A test was done on 09/30/10 to study the effect of tube cooling time on nanomaterial emissions. The FMPS test results are summarized in **Figure 20**. **Figure A-6** presents the measurement results from the APS and DustTrak for reference only, because no large size particles were found. The test clearly demonstrated that the hot and warm tubes resulted in higher particle concentrations (2–3 orders of magnitude greater than background) for a longer time (3–4 minutes), while a long cooling time produced lower nanoparticle emissions (less than 2 orders of magnitude) for a short time period (~1 min). Similar to **Figure 18** and **Figure 19**, the size distribution analysis for this test presented in **Figure 21** confirmed that released nanoparticles were less than 15 nm.

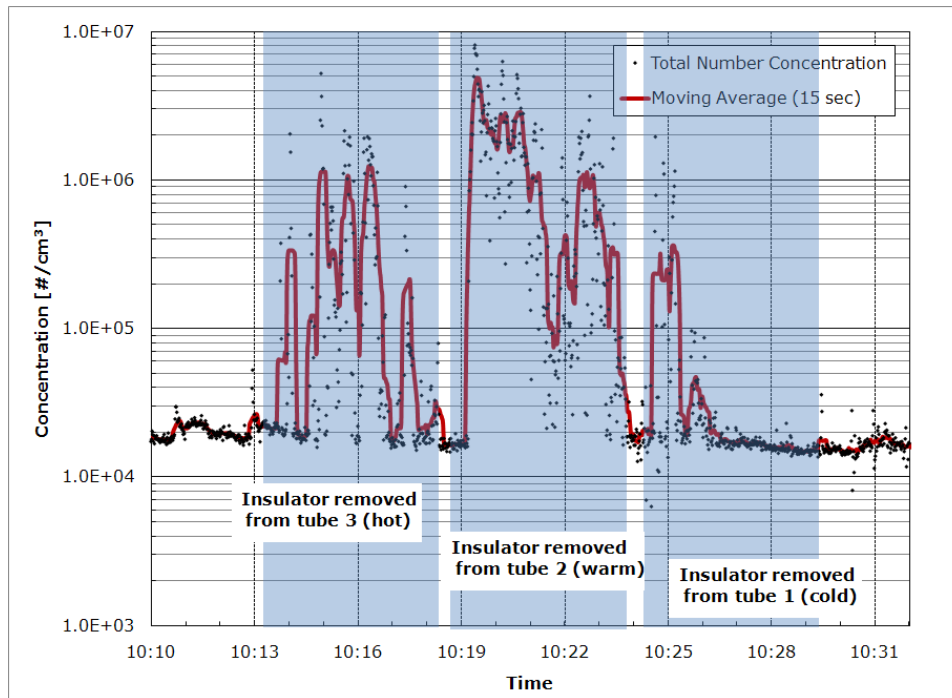


**Figure 20:** Sampling results from the tubes with different cooling time during the post-treatment process as monitored by FMPS on 09/30/10.

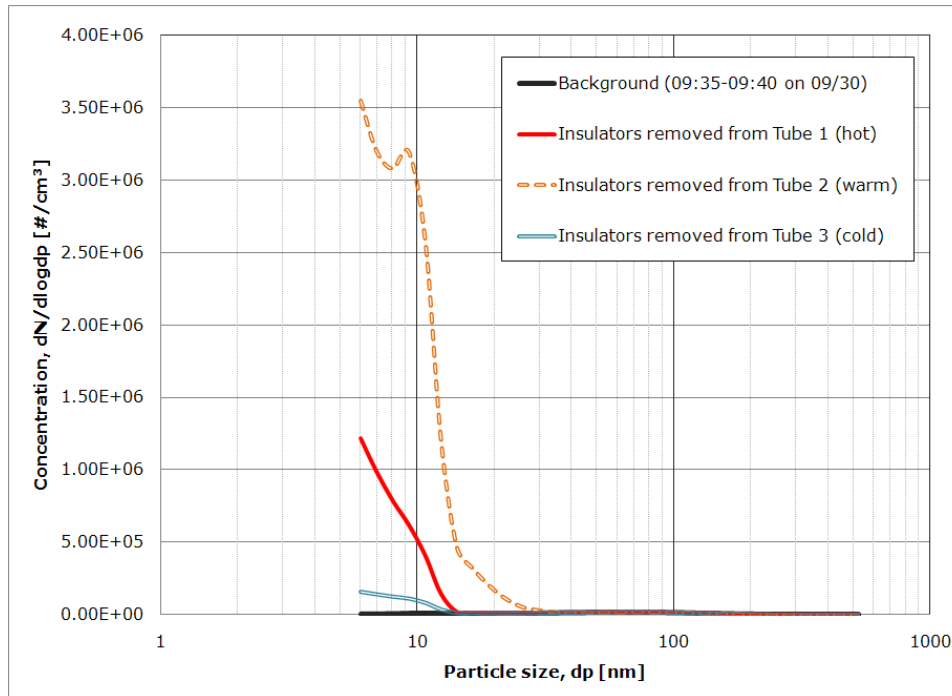


**Figure 21:** Size distribution analysis for the tube cooling time test presented in **Figure 20**.

## Non-Production Areas

### R&D Laboratories

Aerosol monitoring of the R&D laboratories and the office areas were conducted on 09/30/10. Fume hoods and glove boxes were used for most activities in the R&D laboratories. The total particle number concentrations in these laboratory areas were stable as summarized in **Table 3** for the FMPS measurements. The background data measured in the production area near the door of Lab 2 from 11:35 to 13:00 were reported here for reference. The possible reasons for the higher average concentration found in Lab 1 were that workers usually accessed the laboratories with the door in Lab 1, and more activities were conducted in this room than in the other two. The nanoparticle concentrations in the R&D laboratories were 19%–64% higher than the background found in the production areas ( $\sim 1 \times 10^4$  #/cm<sup>3</sup>). The size analysis presented in **Figure 22** for the laboratory areas showed that the aerosols were bimodal distributions with peaks at 10 and 70 nm, and they have similar distributions as background measured outside the Lab 2 door. The background distributions changed from polydisperse (**Figure 9**) in

the morning to bimodal (**Figure 22**) in the afternoon, because of accumulation of nanoparticles  $\sim 10$  nm released from the production processes.

**Table 3.** Summary of aerosol monitoring with the FMPS for laboratories on 09/30/10.

Location	Time	Average total number concentration [ $\#/cm^3$ ]	Standard deviation [ $\#/cm^3$ ]
Background in the production area	11:35–13:00	10255	3388
Lab 3	13:15–13:20	12220	247
Lab 2	13:58–14:07	12813	640
Lab 1	14:08–14:27	16802	463

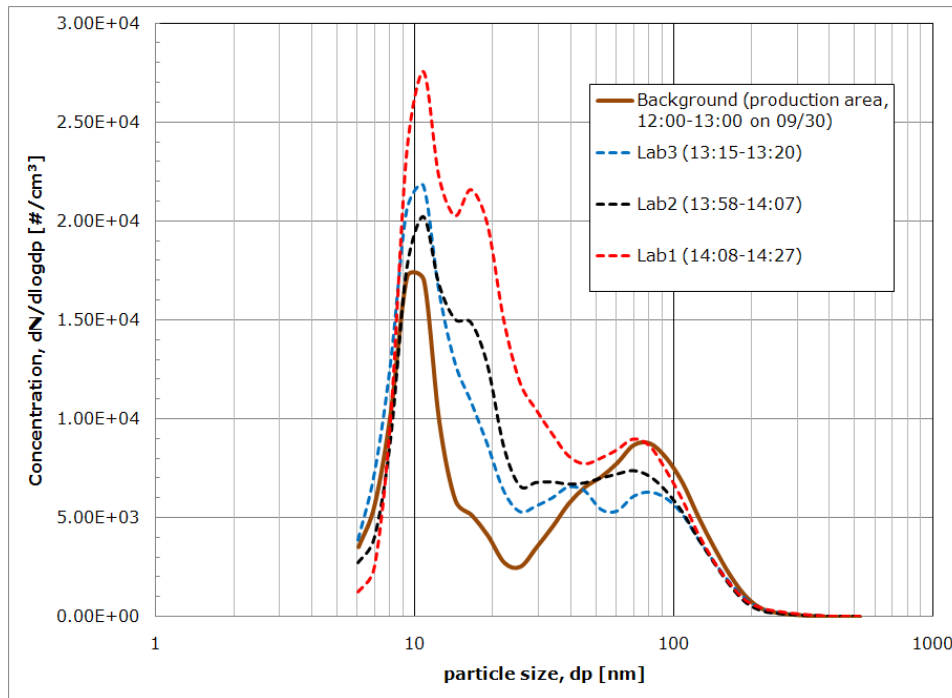
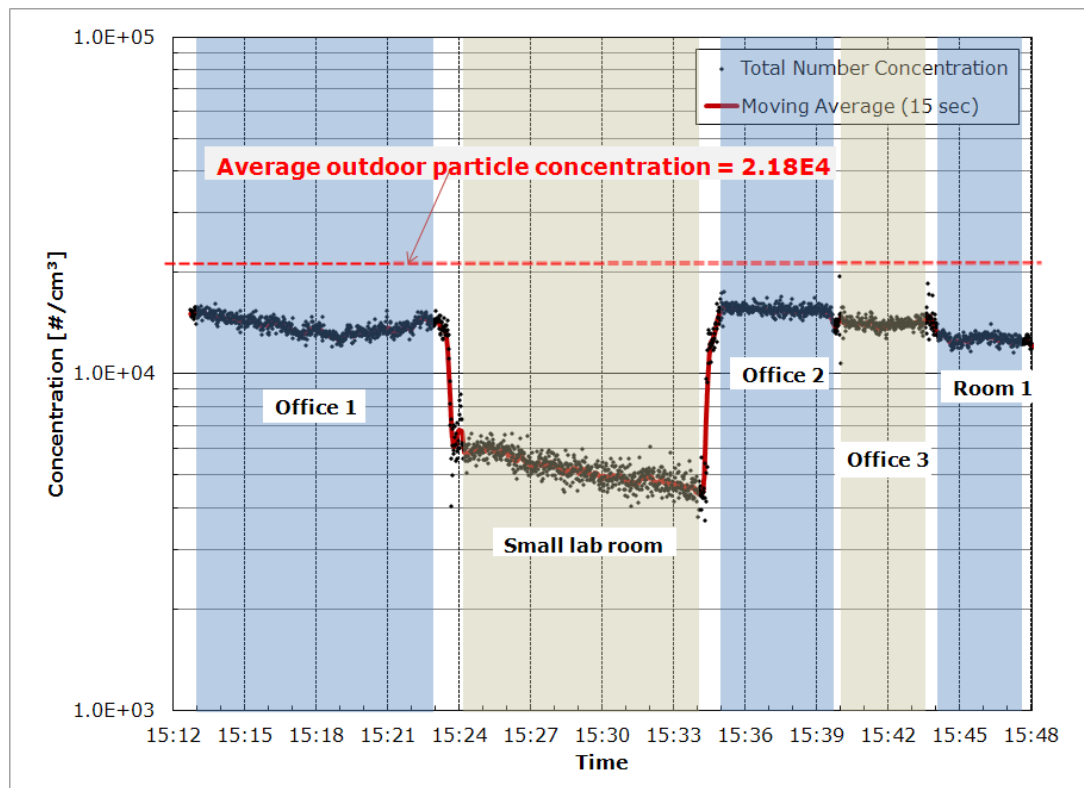


**Figure 22:** Size distributions of R&D laboratories as monitored with the FMPS on 09/30/10.

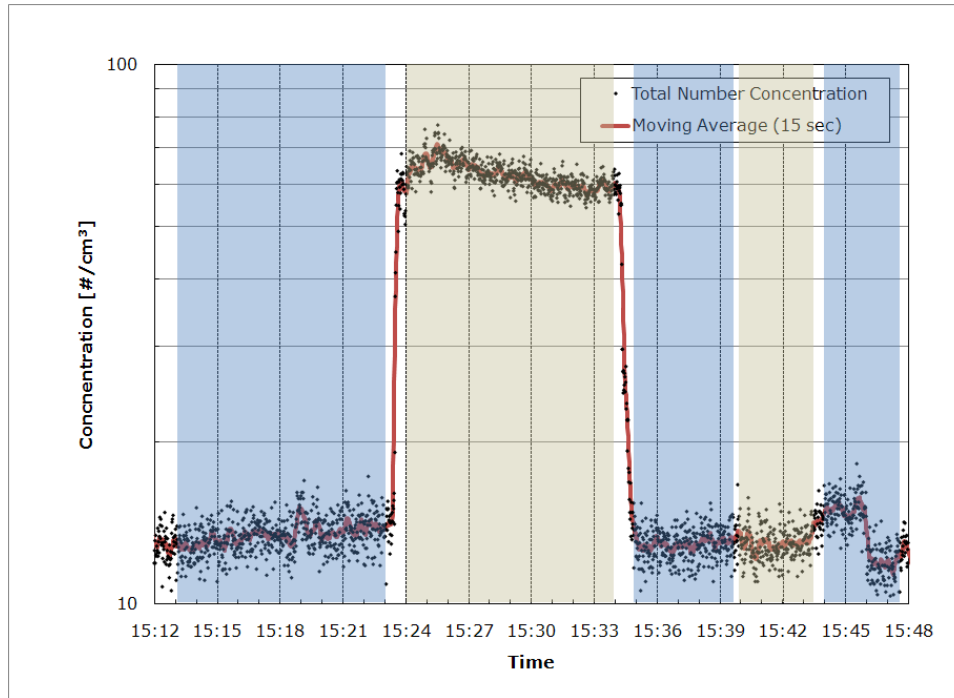
## Offices

The fine particle concentrations found in the office were on the same level as the background concentrations in the production areas (**Figure 23-a**). When the sampling cart was moved to the small lab next to the office area, small particle concentration dropped to half of that found in the office area. The concentration increased to the original level once the sampling instrument was moved to other areas. Compared to other office areas, the small lab was operated at a higher air exchange rate and kept under positive pressure to lower the airborne nanoparticle concentration. However, it was found that the number and mass concentrations of large particles in the small lab were higher than those in other office areas (**Figure 23-b** and **Figure 23-c**). The R&D activities in the small lab could be the main reason causing higher large particle concentrations, though high volume ventilation flow was used to reduce airborne nanoparticles.

(a)



(b)



(c)

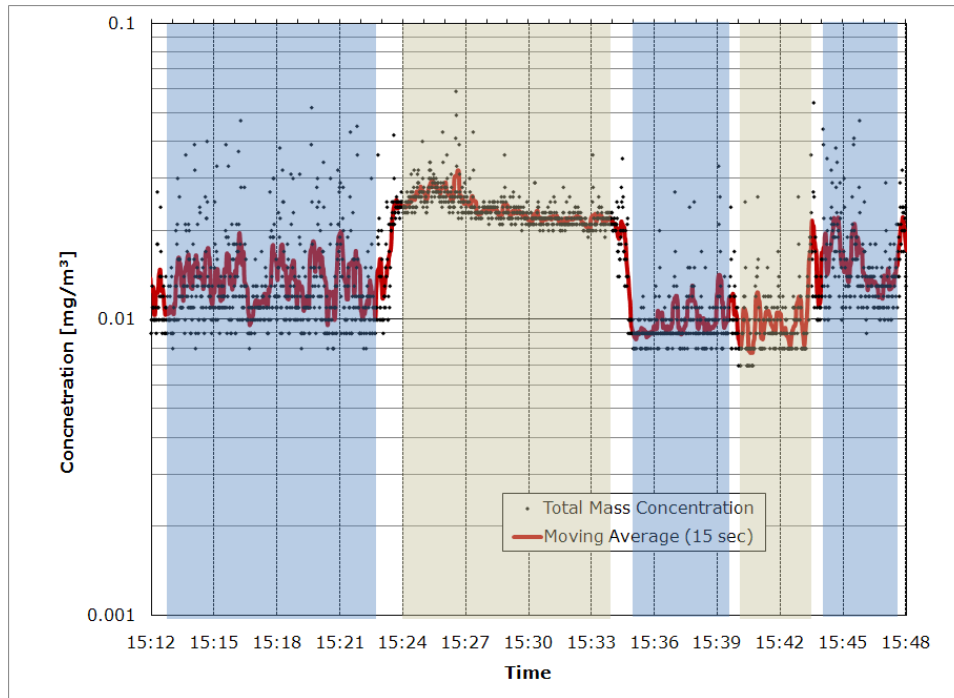


**Figure 23:** Sampling results from the office areas as monitored by (a) FMPS, (b) APS, and (c) DustTrak on 9/30/10

For this nanomanufacturing facility, the greatest concern was the high concentration of fine particles in the non-production areas rather than the increased concentrations of larger particles found only in the small lab. The results of particle size analysis from the FMPS showed that the airborne particles in the office areas (**Figure 24**) were lognormally distributed at 25 nm in Office 1, 35 nm in the small lab and Room 1, and 40 nm in Offices 2 and 3. They were different from those found in the production areas (**Figure 9, Figure 11, Figure 14-a, Figure 18, Figure 19, and Figure 21**) all showing polydisperse distributions. Recall that Office 1 is located next to the production areas, and a door is installed between these two spaces for access. Data from the direct-reading instruments suggested that opening/closing the door did not cause any change in the particle concentrations in Office 1. Therefore, the prevalence of high particle concentrations in the non-production areas could likely be attributed to the plant ventilation system.

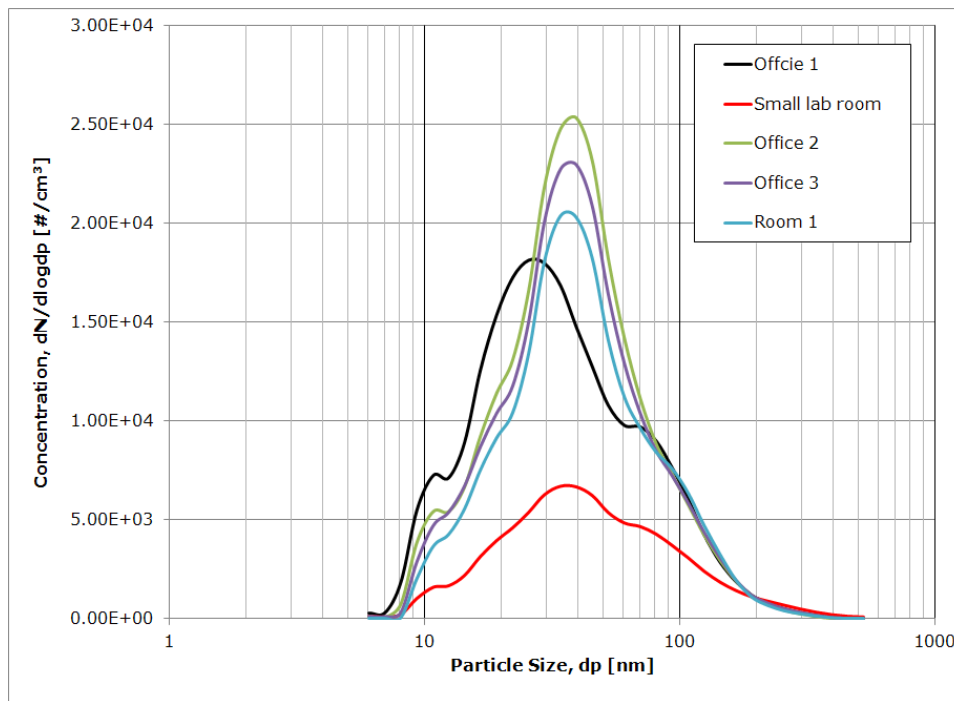


**Figure 24:** Average particle size distributions as measured by the FMPS in the office areas.

## Conclusions and Recommendations

Some tasks in the production areas were identified as the sources of release of nanoparticles into the workplace. They are raw material preparation, product harvesting, and product transfer inside a ventilated enclosure in the refining area, and tube cooling and insulator removal from tubes in the post-treatment area. Appropriate engineering controls could help mitigate exposure to nanomaterials in production areas. A detailed discussion of feasible control measures for exposure control in these identified tasks is provided below. It is also required that workers wear PPE (including respirators, safety glasses, PVC gloves, and work suits with long sleeves) at all times while handling nanomaterials to protect them from contact with these potentially hazardous materials. Detailed information for a respirator protection program and mandatory fit testing can be found at the Occupational Safety and Health Administration website [OSHA].

### Refining Area

#### 1. Raw Material Preparation

Removing raw materials from a drum and mixing the materials with water released particles with diameters of  $1.6 \sim 3 \mu\text{m}$  (**Figure 16**). While PPE may provide adequate protection for workers performing these tasks, a better solution would be flexible enclosures that could prevent releases during removing and mixing of materials and allow easy cleanup of spills.

An example of a flexible enclosure is shown in **Figure 25**. A flexible enclosure separates the processes and the work area. Glove sleeves and an entry/removal access door allow users to easily perform various operations on materials or products. High efficiency particulate air (HEPA) filters are incorporated with the enclosure to balance the inside pressure. The flexible enclosure is moveable for working in different areas. For this study site, the entry/removal door should be modified to accommodate the sizes of the drum and the mixer. The support table may not be necessary in this application because of the size of the drum and the mixer.



**Figure 25:** Flexible enclosure. Main components are marked by numbers: (1) enclosure, (2) HEPA filters, (3) integral glove sleeves, (4) entry/removal door, (5) conductive locking castors, and (6) support table. (Reprint from [ILC Dover, 2009])

## 2. Product Harvesting

Flexible enclosures can also be used to retrofit existing equipment to prevent large particles or agglomerated nanomaterials from dispersing into the workplace during product harvesting. The harvesting area of the process tank can be contained by a flexible enclosure integrated with glove sleeves for accessing the container (**Figure 26**). Exhaust equipped with HEPA filters will be used during product harvesting to mitigate particle emissions.

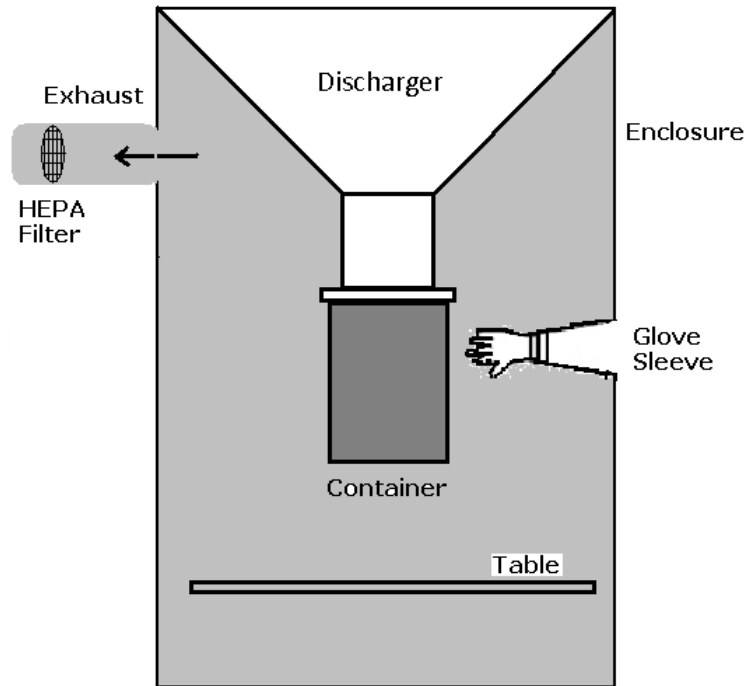


**Figure 26:** Flexible enclosure for product harvesting.

Another feasible solution is to install split butterfly valves between the dischargers and the containers for product harvesting. Split butterfly valves have been widely used in the pharmaceutical industry to transfer products or materials from one process vessel to another. They effectively minimize particle emissions in work areas. The transfer is processed in contained devices when utilizing split butterfly valves.

The operational sequence of a split butterfly valve is illustrated in **Figure 27**. The valve consists of two halves, the active part and the passive part. Each of them presents an ordinary butterfly valve. Typically the active part seals the stationary process equipment such as the discharger in this case, and the passive part is attached to the container. When two halves are docked together to form a single sealed valve (**Figure 27-2**), the valve can be opened manually or automatically to allow the transfer of materials from the vessel to the container (**Figure 27-3**). Once the transfer is completed, the valve is closed and two halves are separated again (**Figure 27-4** and **Figure 27-5**). This technology can eliminate particle emissions (i.e., increase

yield) during product transfer, and reduce the costs associated with cleaning.

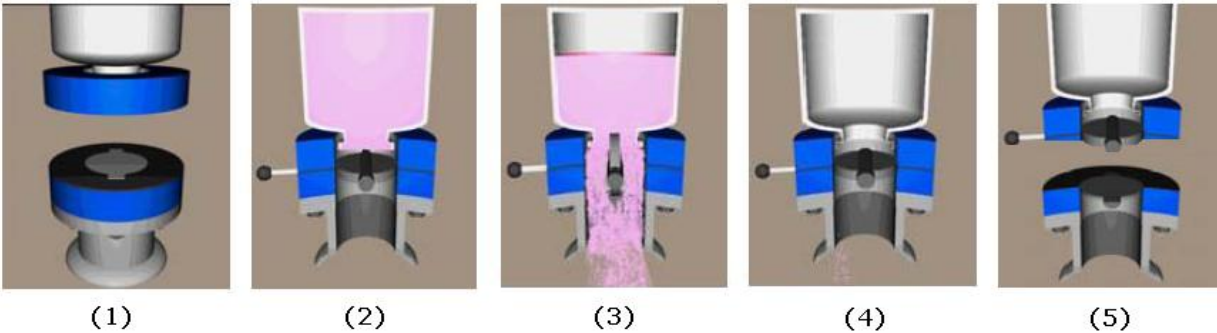


**Figure 27:** Transfer sequence of a typical split butterfly valve (reprint and modification from [Belger, 2011]).

### 3. Product Transfer/Package

Though a ventilated enclosure has been used to transfer and package final products, some large particles were identified around the worker breathing zone by the APS and the DustTrak during material handling inside the enclosure. The existing enclosure was operated at an average face velocity of 78 fpm, and a lower face velocity of 54 fpm was found in the fume hoods in the R&D labs. OSHA specifies that hood face velocity should be approximately 60–100 linear feet per minute [CFR 1910.1450 App A]. The Industrial Ventilation manual Table 6-2 recommends 75–100 fpm for processes with little motion [ACGIH, 2010]. Therefore, higher air velocities are recommended to provide good containment, though the average face velocity of the enclosure meets both criteria. The average face velocity of the enclosure can reach 182 fpm when the door is lowered. Lowering the enclosure door to adjust the open area (to increase face velocity) should help reduce worker exposure to nanomaterials during the operation.

To protect workers, HEPA filtered enclosures are recommended for handling nanomaterials. A routine certification program should be established to monitor filter life and face velocity to assure that the filter performs as designed.

## Post-Treatment Area

Very high concentrations of small particles were measured by the FMPS from the post-treatment process. The FMPS size analysis showed that most particles are less than 15 nm. As shown in this study, extending the cooling time of the tubes may help lower particle emissions, but high concentrations of nanoparticles were still released to the work area. The only installed control measure for the process is a 4" diameter local exhaust flexible duct operated at an average velocity of 1105 fpm (volume flow rate of 96 cfm) on the top of the reactor (**Figure 4**). In addition to insufficient airflow, it does not have a receiving hood to effectively capture nanoparticle emissions.

As shown in **Figure 28**, a better solution for the post-treatment area is to modify an existing canopy hood (**Figure 5**) positioned above the reactor and the harvest area. The vertical height of a canopy hood above the reactor should not exceed 3 ft to ensure the control efficiency. The horizontal distance between the rims of the hood opening and the edges of workbench should not be less than 1 ft. The hood exhaust rate should be equal to the induced hot air flow rate plus an additional flow rate sufficient to prevent air from escaping out of the hood space. Operating a canopy hood at face velocities of 100 to 150 fpm may be adequate in most cases where room air turbulence is not excessive [Hemeon, 1999]. The efficiency of a canopy hood can be improved by adding baffle plates. Baffle plates can reduce the net open area to minimize the hood exhaust rate required and prevent tidal surges and spillage of interior air. A canopy hood with side walls can provide better containment to further improve the control efficiency.

For this process, the canopy hood should be designed to capture the angle of the convection current plume and to overcome the velocities generated by the convection current plume. It should also be designed to eliminate the possibility of drawing the contaminants across the workers breathing zone.

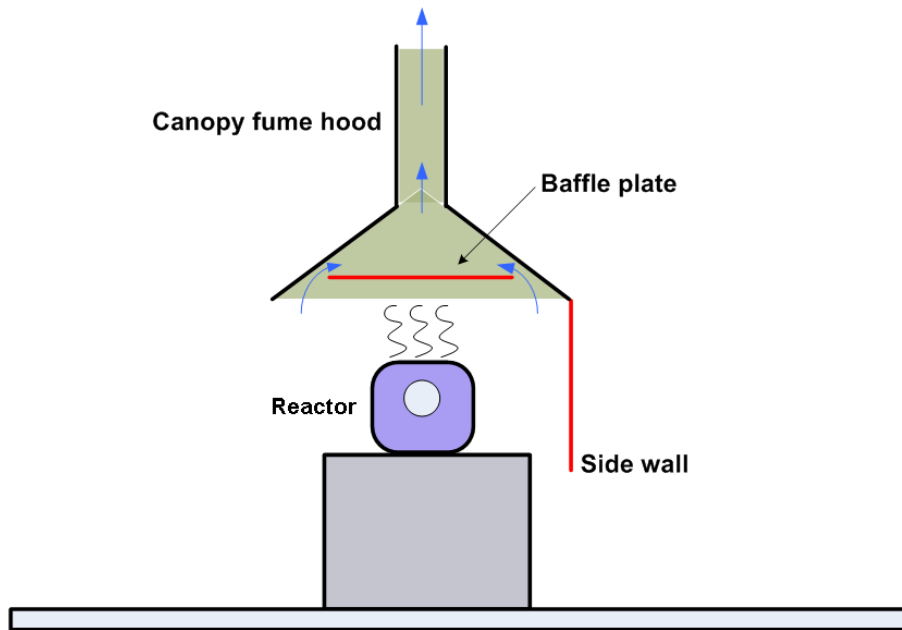


**Figure 28:** Canopy hood for the post-treatment process. The efficiency of a canopy fume hood can be improved by adding a baffle plate and side walls.

An isolated work area is another option for the post-treatment process. A downflow booth shown in **Figure 29** is a good engineering control that achieves containment by providing unidirectional HEPA filtered airflow typically 90 fpm when measured at 3 ft from the diffuser screen over the process zone [Floura & Kremer, 2008]. An open front design allows easy access for both personnel and materials. Contaminants released from the processes are removed by downward air flow and captured on pre-filters and HEPA filters. The filtered air is usually re-circulated to the supply plenum to create a push-and-pull flow pattern. The booth will also allow a bleed out of filtered air if air comes into the booth when the front curtain is open for access.

Considering the procedures and the operating conditions in this case, a downflow booth is a feasible solution to mitigate air containments released from this process. To maintain unidirectional airflow, the downflow booth would have to be designed with enough flow to overcome the velocity of the convection currents coming off of the process reactor before they reach the worker's breathing zone.

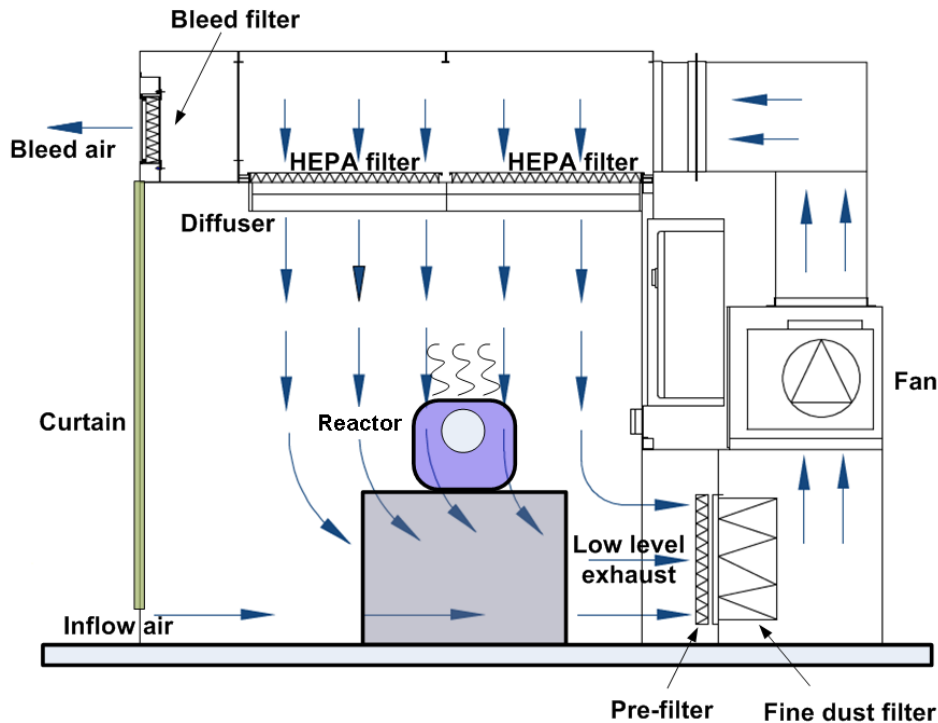


**Figure 29:** Downflow booth providing unidirectional HEPA filtered airflow. (modified from Esco Pharmacon Downflow Booth [Esco Technologies Inc., 2009])

## Non-Production Areas

The background concentrations in the production areas and the non-production areas were similar in total number of fine particles. This finding indicated that the ventilation system may be a key factor to improve the air quality of the facility. The existing ventilation system should be assessed, and if necessary, modified for better environmental control. The ventilation system is used to supply dilution air by bringing outdoor air into the space and remove air containments generated from processes by exhaust air systems. For general ventilation, the replacement airflow rate should be slightly more than the total exhaust flow rate. In the non-production areas, adequate dilution volumes and suitable air filtration can lower the risk of office workers' exposure to nanomaterials generated from the production area.

A positive air pressure differential should be maintained for the non-production areas with respect to adjacent production areas. A good performance standard for industrial processes is to set a pressure differential of  $0.04 \pm 0.02$  inches of H<sub>2</sub>O [ACGIH, 2010]. This helps reduce the potential escape of nanomaterials from production areas and exposure to office and other workers. To maintain a slight pressure difference, the room supply air volume in the production areas should be less than the exhaust air. A general guide is to set a 5% flow difference between supply and exhaust flow rates but no less than 50 cfm [ACGIH, 2010].

The performance of air filters is affected by the aerosol characteristics including particle size, shape, concentration, and electrical properties. The ASHRAE handbook lists air filters classified according to their efficiencies and types as guidance for different applications [ASHRAE, 2008]. These air filters should be routinely checked by monitoring the pressure drop, and replaced when high resistance is detected.

## **Acknowledgements**

The authors would like to acknowledge study support from Mr. Carlos Crawford, Ms. Catherine Beaucham, and Dr. Mark Methner (NIOSH NTRC Field Team) for collecting air filter samplers. The results of TEM analysis and elemental carbon analysis for the samples are summarized in their letter report. The authors also wish to acknowledge the support and cooperation from the management and staff of the study site. We also appreciate the draft report review from Dr. Scott Earnest, Mr. Ronald Hall, Dr. Michael Gressel, and Mr. Kenneth Martinez and editorial comments from Ms. Ellen Galloway.

## References

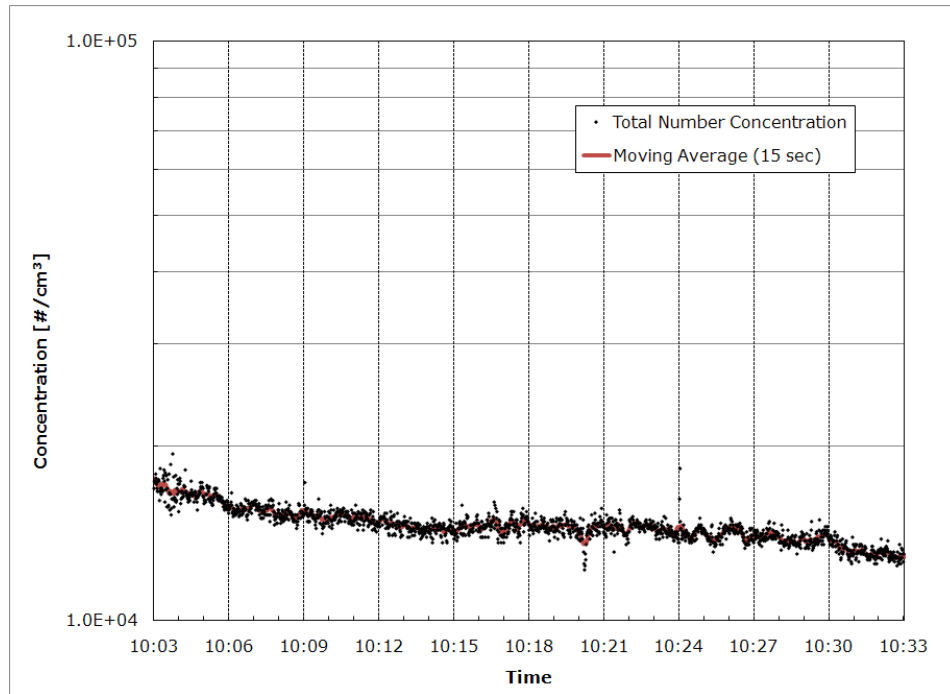
- ACGIH. (2010). *Industrial ventilation: a manual of recommended practice for design* (27th ed.). Cincinnati, Ohio.: American Conference of Governmental Industrial Hygienists.
- ACGIH. (2011). *TLVs and BEIs*: American Conference of Governmental Industrial Hygienists.
- ANSI/ASHRAE 110-1995 Standard. (1995). Method of testing performance of laboratory fume hoods
- ASHRAE. (2008). *ASHRAE handbook: HVAC systems and equipment*
- Belger, T. (2011). Split butterfly valve technology for continuous containment of complete pharmaceutical/chemical process, from <http://www.maintenanceonline.org/maintenanceonline/?page=articles.asp&iid=4202>
- Bello, D., Wardle, B. L., Yamamoto, N., Guzman deVilloria, R., Garcia, E. J., Hart, A. J., Ahn, K., Ellenbecker, M. J., & Hallock, M. (2009). Exposure to nanoscale particles and fibers during machining of hybrid advanced composites containing carbon nanotubes. *J. Nanopart. Res.*, 11(1), 231-249.
- Brouwer, D. K., Gijsbers, J. H. J., & Lurvink, M. W. M. (2004). Personal exposure to ultrafine particles in the workplace: exploring sampling techniques and strategies. *Ann. Occup. Hyg.*, 48(5), 439-453.
- BSI. (2007). Nanotechnologies - Part 2: Guide to safe handling and disposal of manufactured nanomaterials. *PD 6699-2:2007*: British Standards Institution.
- Buzea, C., Blandino, I. I. P., & Robbie, K. (2007). Nanomaterials and nanoparticles: sources and toxicity. *Biointerphases*, 2 (4), MR17-MR172. doi: DOI 10.1116/1.2815690
- CFR 1910.1450 App A. *Code of Federal Regulations, Title 29 Chapter XVII part 1910 Subpart Z Section 1910.1450 Appendices A.*
- Cheekati, S. L., Xing, Y., Zhuang, Y., & Huang, H. (2010). *Nano-graphene platelets and their composites for Li-ion batteries*. Paper presented at the 218th ECS Meeting, Las Vegas, Nevada.
- Esco Technologies Inc. (2009). Pharmacon downflow booth, from [http://us.escoglobal.com/PDF/DFB\\_sellsheet.pdf](http://us.escoglobal.com/PDF/DFB_sellsheet.pdf)
- European Agency for Safety and Health at Work. (2009). Literature review: workplace exposure to nanoparticles. 89 pages.

- Evans, D. E., Ku, B. K., Birch, M. E., & Dunn, K. H. (2010). Aerosol monitoring during carbon nanofiber production: mobile direct-reading sampling. *Ann. Occup. Hyg.*, 54(5), 514-531.
- Floura, H., & Kremer, J. (2008). Performance verification of a downflow booth via surrogate testing. *Pharmaceutical Engineering*, 28(6), 9 pp.
- Heine, T., Zhechkov, L., & Seifert, G. (2004). Hydrogen storage by physisorption on nanostructured graphite platelets. *Phys. Chem. Chem. Phys.*, 6, 980-984.
- Hemeon, W. C. L. (1999). Chapter 8: Exhaust for Hot Processes. In D. J. Burton (Ed.), *Hemeon's Plant & Process Ventilation* (3rd ed.): Lewis Publishers.
- ICON. (2006). A survey of current practices in the nanotechnology workplace: condensed report. *International Council on Nanotechnology*, 52 pages.
- ILC Dover. (2009). Flexible containment technology, from <http://www.pharmaceutical-int.com/article/flexible-containment-technology.html>
- International Organization for Standardization. (2008). Nanotechnologies -- Health and safety practices in occupational settings relevant to nanotechnologies. *ISO/TR 12885:2008*, 79 pages.
- Jang, B. Z., & Zhamu, A. (2008). Processing of nanographene platelets (NGPs) and NGP nanocomposites: a review. *J Mater Sci*, 43, 5092-5101.
- Kim, J. Y., Magari, S. R., Herrick, R. F., Smith, T. J., & Christiani, D. C. (2004). Comparison of fine particle measurements from a direct-reading instrument and a gravimetric sampling method. *J Occup. Environ. Hyg.*, 1(707-715).
- Lehocky, A., & Williams, P. L. (1996). Comparison of respirable samplers to direct-reading real-time aerosol monitors for measuring coal dust. *Am. Indus. Hyg. Assoc. J.*, 57, 1013-1018.
- Mark, D. (2007). Occupational exposure to nanoparticles and nanotubes. In R. E. Hester & R. M. Harrison (Eds.), *Nanotechnology: consequences for human health and the environment* (pp. 50-80): RSC Publishing.
- OSHA. Personal Protective Equipment, from [http://www.osha.gov/pls/oshaweb/owadisp.show\\_document?p\\_id=12716&p\\_table=standards](http://www.osha.gov/pls/oshaweb/owadisp.show_document?p_id=12716&p_table=standards) (respirator protection)  
[http://www.osha.gov/pls/oshaweb/owadisp.show\\_document?p\\_table=STANDARDS&p\\_id=9780](http://www.osha.gov/pls/oshaweb/owadisp.show_document?p_table=STANDARDS&p_id=9780) (fit testing)
- OSHA. Standards - 29 CFR PART 1910 Occupational Safety and Health Standards: Occupational Safety & Health Administration.

- Peters, T. M., Elzey, S., Johnson, R., Park, H., Grassian, V. H., Maher, T., & O'Shaughnessy, P. (2009). Airborne monitoring to distinguishing engineered nanomaterials from incidental particles for environmental health and safety. *J. Occup Environ. Hyg.*, 6, 73-81.
- Rafiee, M., Rafiee, J., Wang, Z., Song, H., Yu, Z. Z., & Korakar, N. (2009). Enhanced mechanical properties of nanocomposites at low graphene content. *ACS Nano*, 3(12), 3884-3890.
- Safe Work Australia. (2009a). Engineered nanomaterials: a review of the toxicology and health hazards. 163 pages.
- Safe Work Australia. (2009b). Engineered Nanomaterials: Evidence on the Effectiveness of Workplace Controls to Prevent Exposure. 75 pages.
- Tsai, S.-J., Ada, E., Isaacs, J. A., & Ellenbecker, M. J. (2009). Airborne nanoparticle exposures associated with the manual handling of nanoalumina and nanosilver in fume hoods. *J Nanopart res*, 11, 147-161.
- TSI Inc. (2008). Mass concentration comparison between the DustTrak DRX aerosol monitor and TEOM. *TSI Application Note EXPMN-004*, 5 pages.
- Watcharotone, S., Dikin, D. A., Stankovich, S., Piner, R., Jung, I., Dommett, G. H. B., Evmenenko, G., Wu, S. E., Chen, S. F., Liu, C. P., Nguyen, S. T., & Ruoff, R. S. (2007). Graphene-silica composite thin films as transparent conductors. *Nano Letters*, 7(7), 1888-1892.
- Yang, K., Wan, J., Zhang, S., Zhang, Y., Lee, S. T., & Liu, Z. (2011). In vivo pharmacokinetics, long-term biodistribution, and toxicology of PEGylated graphene in Mice. *ACS Nano*, 5(1), 516-522.

# Appendixes

(a)



(b)

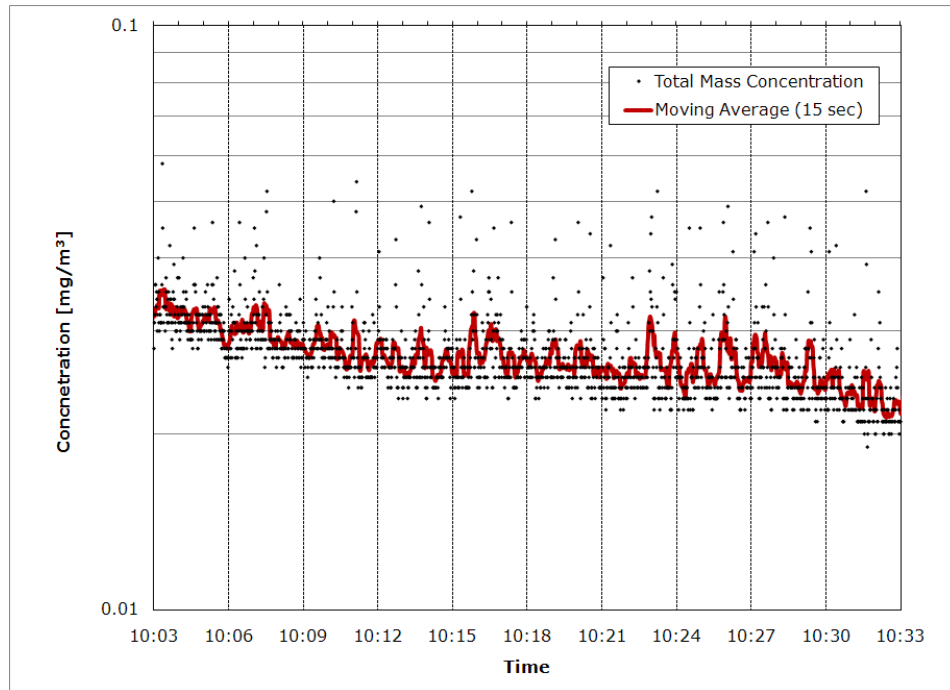
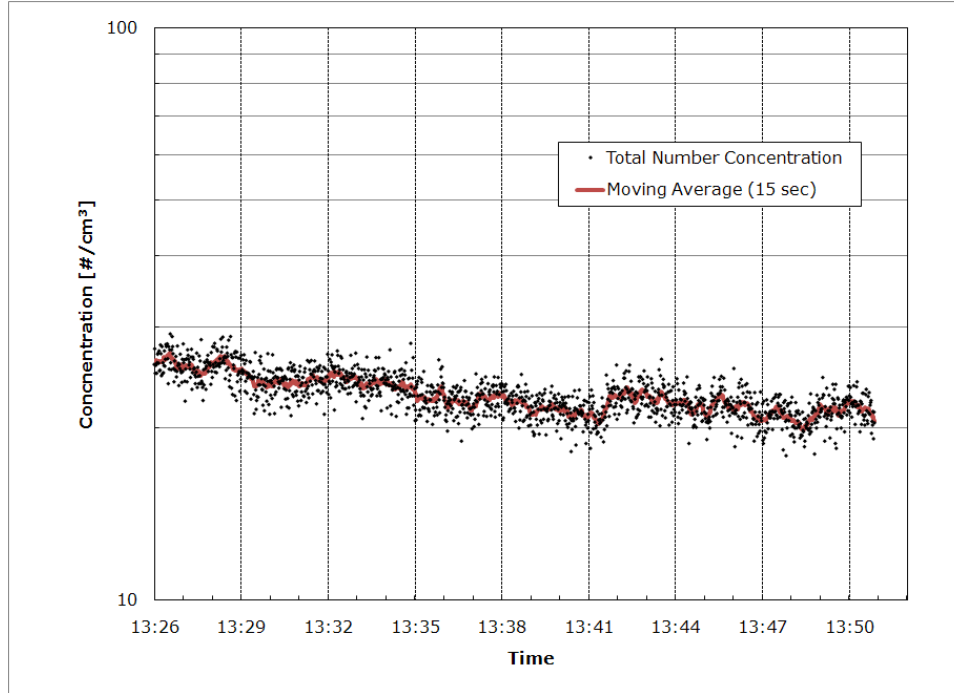


**Figure A-1:** Area monitoring data measured by (a) FMPS and (b) DustTrak in Location AM1 on 09/29/2010.

(a)



(b)

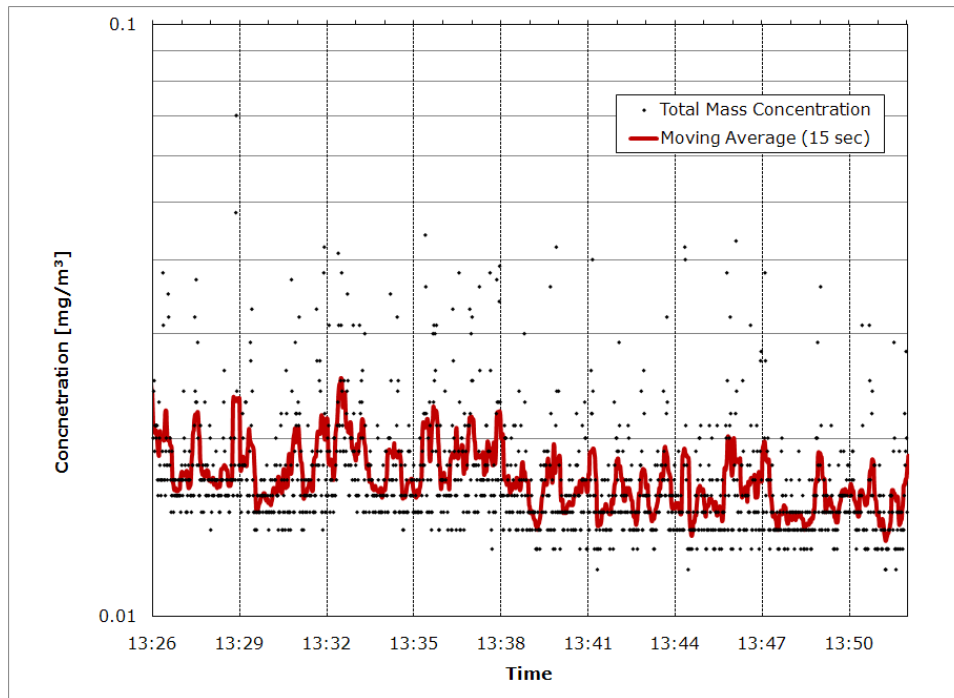
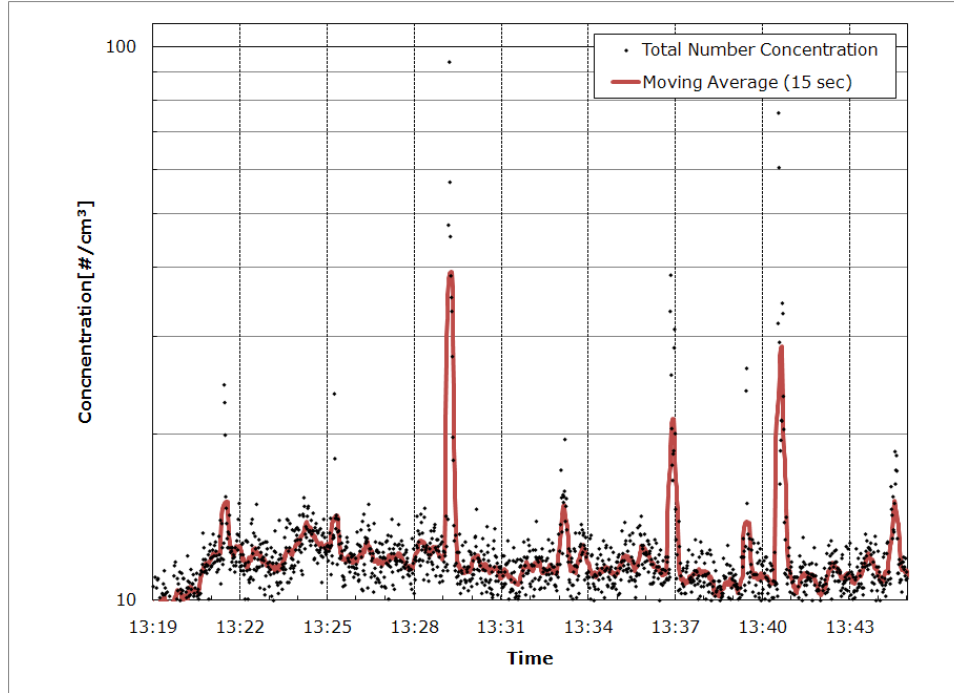


**Figure A-2:** Particles released from the compressor as measured by (a) APS and (b) DustTrak on 09/29/2010.

(a)



(b)

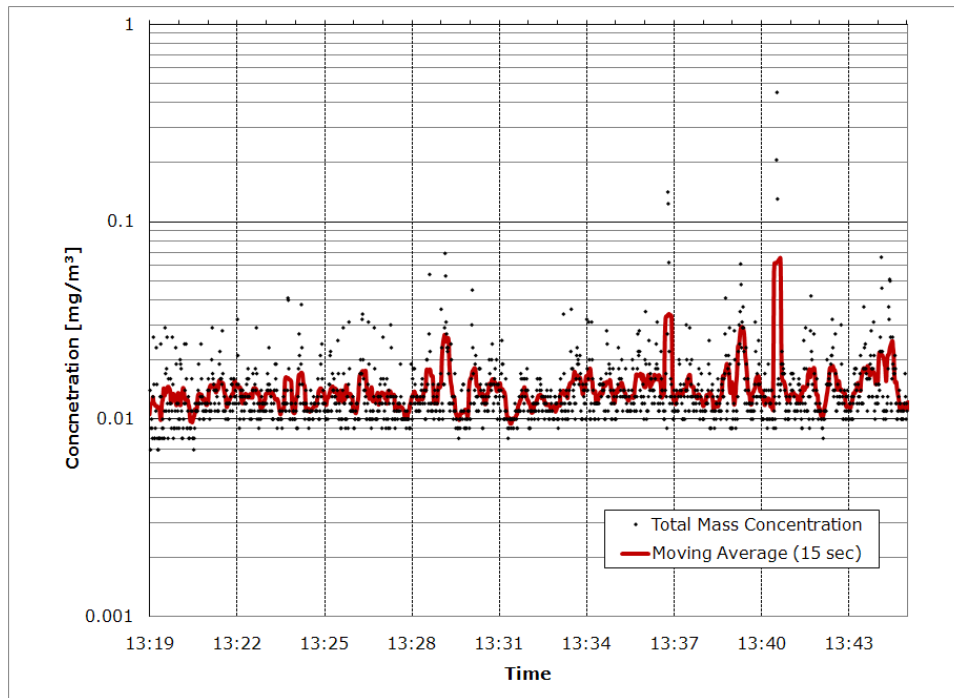
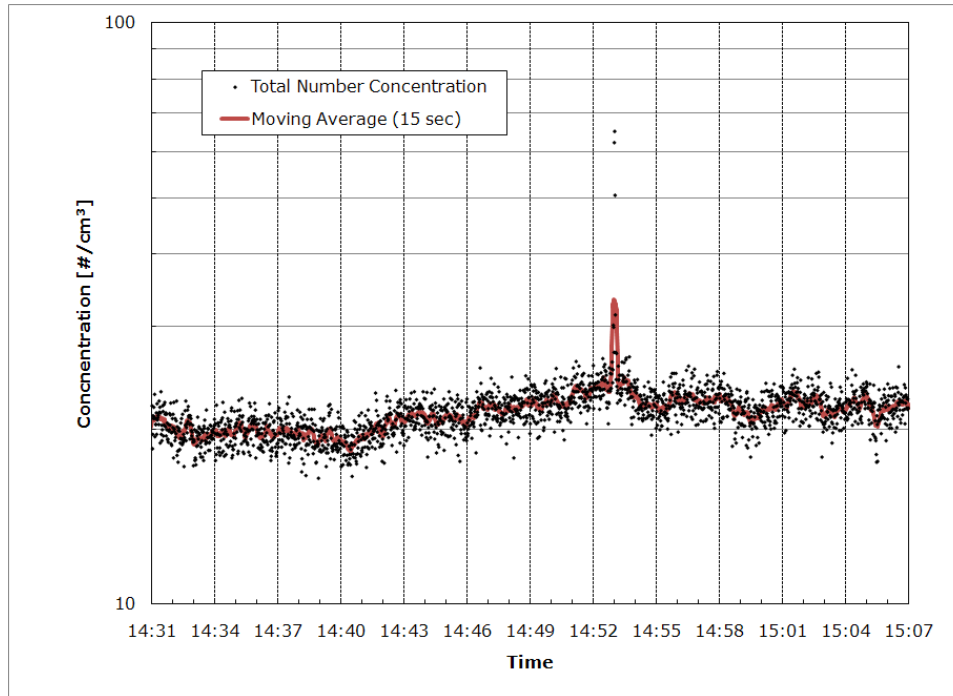


**Figure A-3:** Particles released from the compressor as measured by (a) APS and (b) DustTrak on 09/30/2010.

(a)



(b)

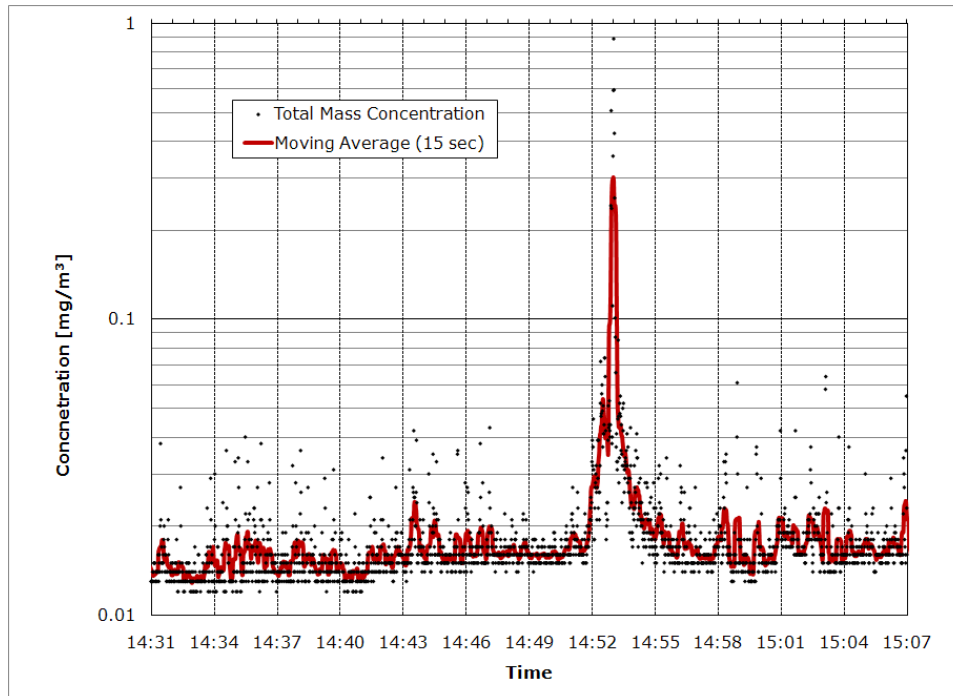
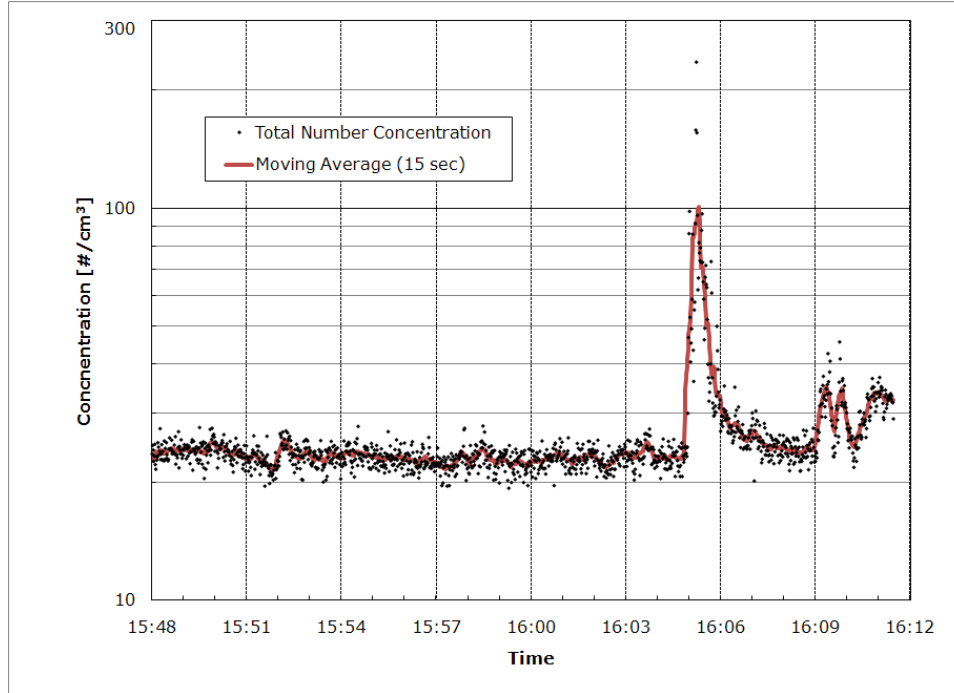


**Figure A-4:** Sampling results of Test 1 from (a) APS and (b) DustTrak for the post-treatment process on 09/29/2010.

(a)



(b)

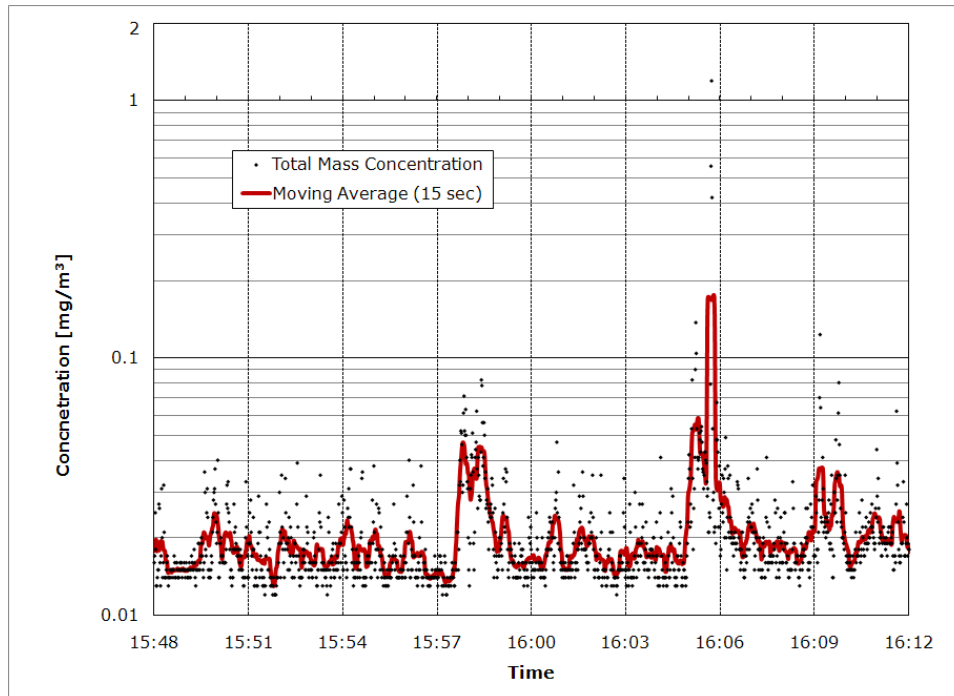
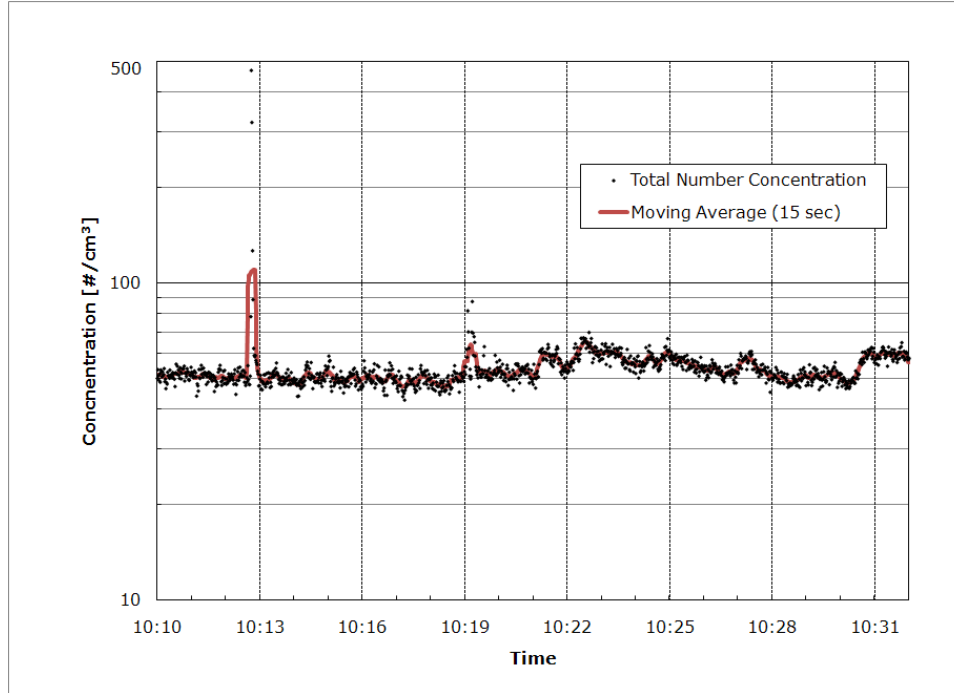


**Figure A-5:** Sampling results of Test 2 from (a) APS and (b) DustTrak for the post-treatment process on 09/29/2010.

(a)



(b)

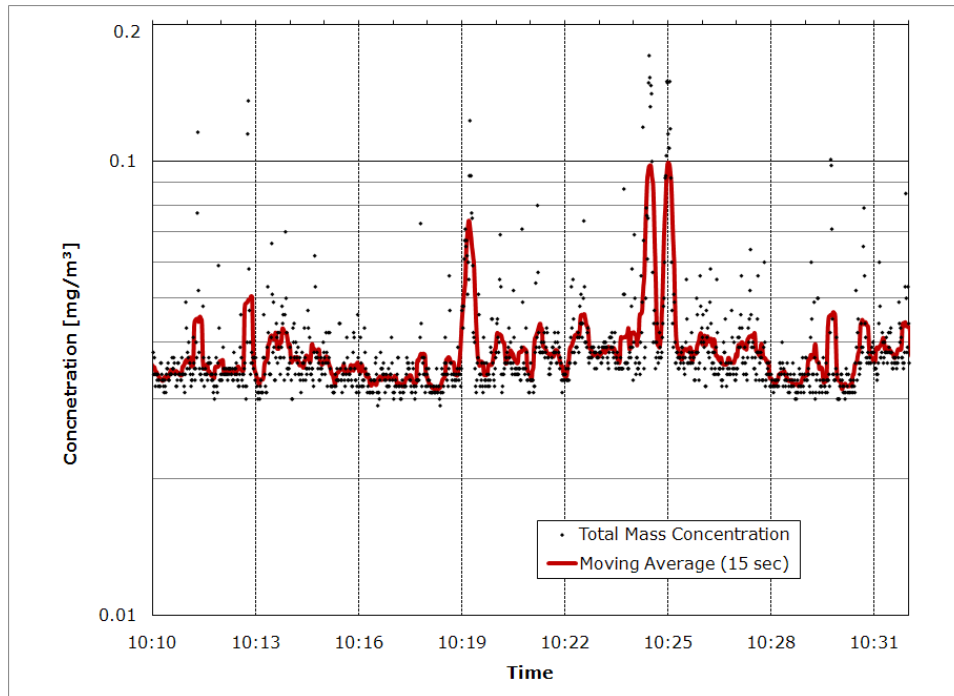


**Figure A-6:** Sampling results of evaluating the effect of tube cooling time as measured by (a) APS and (b) DustTrak on 09/30/2010.



**Delivering on the Nation's promise:  
Safety and health at work for all people  
through research and prevention.**

**To receive NIOSH documents or other information about  
occupational safety and health topics, contact NIOSH at**

**1-800-CDC-INFO (1-800-232-4636)**

**TTY: 1-888-232-6348**

**E-mail: [cdcinfo@cdc.gov](mailto:cdcinfo@cdc.gov)**

**or visit the NIOSH Web site at [www.cdc.gov/niosh](http://www.cdc.gov/niosh)**

**For a monthly update on news at NIOSH, subscribe to  
NIOSH eNews by visiting [www.cdc.gov/niosh/eNews](http://www.cdc.gov/niosh/eNews)**

**SAFER • HEALTHIER • PEOPLE**